

AIRE OLESK

Hemiboreal Forest Mapping with  
Interferometric Synthetic Aperture Radar





## AIRE OLESK

Hemiboreal Forest Mapping with  
Interferometric Synthetic Aperture Radar



This study was carried out at the University of Tartu, Tartu Observatory, AS Regio/Reach-U and European Space Agency (ESA).

The dissertation was admitted on September 6, 2016 in partial fulfilment of the requirements for the degree of Doctor of Philosophy in Physics, and was allowed for defence by the Council of the Institute of Physics, University of Tartu.

Supervisors: DSc Mart Noorma, University of Tartu, Estonia  
DSc Jaan Praks, Aalto University, Finland  
PhD Kaupo Voormansik, Tartu Observatory, Estonia

Opponents: PhD Svein Solberg, Norwegian Institute of Bioeconomy  
Research, Norway  
PhD Rivo Uiboupin, Tallinn University of Technology, Estonia

Defence: November 23, 2016, at the University of Tartu

The research presented in this thesis was supported by the Foundation Archimedes DoRa T3 scholarship.



ISSN 1406-0647  
ISBN 978-9949-77-245-2 (print)  
ISBN 978-9949-77-246-9 (pdf)

Copyright: Aire Olesk, 2016

University of Tartu Press  
[www.tyk.ee](http://www.tyk.ee)

# CONTENTS

LIST OF ORIGINAL PUBLICATIONS .....	6
AUTHOR'S CONTRIBUTION TO THE PUBLICATIONS.....	7
ABBREVIATIONS .....	8
1. INTRODUCTION .....	10
1.1. Background .....	10
1.2. Thesis objectives and progress of this work.....	15
2. INTERFEROMETRIC COHERENCE FOR FOREST HEIGHT RETRIEVAL .....	17
2.1. Radar scattering mechanisms in forest.....	17
2.2. Interferometric SAR measurements of forests .....	18
2.3. Modelling SAR coherence for forest .....	22
2.3.1. The Random Volume over Ground model .....	22
2.3.2. Simplified coherence models for forests .....	23
3. SEASONAL AND ENVIRONMENTAL EFFECTS IN FOREST HEIGHT ESTIMATION [Publications I and II] .....	26
3.1. Study area and data .....	26
3.2. Seasonal dynamics .....	28
3.2.1. Impact of temperature and water content changes on coherence.....	28
3.2.2. Effects of foliage seasonal variation on coherence .....	30
3.2.3. Effect of flooded forest floors on coherence .....	31
4. CHARACTERIZATION OF HEMIBOREAL FORESTS USING INSAR COHERENCE MODELS [Publications III and IV].....	33
4.1. Stand height relative to Height of Ambiguity .....	33
4.2. Performance of the interferometric coherence models.....	33
4.3. Effect of tree species on the fit.....	38
4.4. Model fitting dynamics related to the baseline .....	39
4.5. Comparison of the models.....	40
5. CONCLUSION AND FUTURE WORK .....	41
REFERENCES.....	43
SUMMARY .....	52
KOKKUVÕTE (SUMMARY IN ESTONIAN) .....	53
ACKNOWLEDGEMENTS .....	54
PUBLICATIONS.....	57
ERRATA.....	110
CURRICULUM VITAE .....	111
CURRICULUM VITAE IN ESTONIAN.....	114

## LIST OF ORIGINAL PUBLICATIONS

This thesis is based on the following publications (full texts included at the end of the thesis), which are referred to in the text by their Roman numerals. The articles are reprinted with the kind permission of the publishers.

- I A. Olesk, K. Voormansik, A. Vain, M. Noorma and J. Praks, “Seasonal differences in forest height estimation from interferometric TanDEM-X coherence data,” *IEEE Journal of Selected Topics in Applied Earth Observations and Remote Sensing*, vol. 8, no. 12, pp. 5565–5572, 2015.
- II A. Olesk, K. Voormansik, T. Tamm, M. Noorma, and J. Praks, “Seasonal effects on the estimation of height of boreal and deciduous forests from interferometric TanDEM-X coherence data,” In *Proceedings of the SPIE Remote Sensing*, International Society for Optics and Photonics, pp. 964406–964406, 2015.
- III J. Praks, A. Olesk, K. Voormansik, O. Antropov, K. Zalite and M. Noorma, “Building blocks for semi-empirical models for forest parameter extraction from interferometric X-band SAR images,” In *Proceedings of the International Geoscience and Remote Sensing Symposium (IGARSS)*, IEEE International, pp. 736–739, 2016.
- IV A. Olesk, J. Praks, O. Antropov, T. Arumäe, K. Zalite and K. Voormansik, “Interferometric SAR Coherence Models for Characterization of Hemiboreal Forests using TanDEM-X Data,” *Remote Sensing*, vol. 8, no. 12, pp. 700, 2016.

## **AUTHOR'S CONTRIBUTION TO THE PUBLICATIONS**

The publications in this thesis are a result of essential contribution by the author and contain important contributions from all of the co-authors. The Roman numerals refer to the list of publications above, with the author's contribution then described.

- I** This work was mainly done by the author (A. Olesk), who performed the processing of the interferometric SAR data, generated forest stand height map from the LiDAR data and prepared all auxiliary data. The author also carried out data analysis, generated all the figures and wrote the full text of the article. The design of the experiments and interpretation of the results was completed together with Kaupo Voormansik. The work with the forest height modelling was done jointly with Jaan Praks from Aalto University. Co-authors contributed also in editorial work.
- II** This publication was mainly prepared by the author and is an elaboration of the study done in Publication I. The author is responsible for all SAR and reference data processing, analysis and interpretation. The author also designed the structure of the paper and wrote the full text. Interpretation of the results and editorial work was done jointly with the co-authors.
- III** This work was a collaborative effort and preparation for the study that continues in Publication IV. The interferometric coherence and reference data processing are based on Publications I and II and were performed by the author, who was also involved in writing and preparing the article. The first author (J. Praks) carried out the SAR coherence model calculations and prepared the figures. All authors participated in the analysis and interpretation of the results.
- IV** This work was a collaborative effort with Jaan Praks from Aalto University and Oleg Antropov from VTT Technical Research Centre of Finland. The author prepared and processed all the SAR and reference data and conceived and designed the experiments jointly with Jaan Praks and Kaupo Voormansik. LiDAR-derived forest height map was prepared in cooperation with Tauri Arumäe. Jaan Praks and Oleg Antropov performed the experiments. The full text was written by the author, Jaan Praks and Oleg Antropov. All authors analysed the results and revised the paper.

# ABBREVIATIONS

## List of acronyms

AGB	Above ground biomass
ALS	Airborne laser scanning
ASAR	Advanced Synthetic Aperture Radar
C-band	4 to 8 GHz electromagnetic spectrum frequency range
CoSSC	Coregistered Single look Slant range Complex
DEM	Digital elevation model
DLR	German Aerospace Centre
DTM	Digital terrain model
ERS	European remote sensing satellite
ESA	European Space Agency
GCP	Ground control point
GSV	Growing stock volume
HH	Horizontal polarization transmit and horizontal polarization receive
HoA	Height of ambiguity
InSAR	Interferometric SAR
L-band	1 to 2 GHz electromagnetic spectrum frequency range
L-EST	Lambert conformal conic projection, Estonian coordinate system
LiDAR	Light detection and ranging
NESZ	Noise equivalent sigma zero
P-band	0.3 to 1 GHz electromagnetic spectrum frequency range
PolInSAR	Polarimetric interferometric SAR
RMSD	Root-mean-square deviation
RVoG	Random volume over ground
SAR	Synthetic aperture radar
SL	Spotlight mode
SLC	Single look complex
SM	Stripmap mode
SNR	Signal-to-noise ratio
SRTM	Shuttle Radar Topography Mission
TanDEM-X	TerraSAR-X add-on for Digital Elevation Measurements
TDX	TanDEM-X
TBDF	Temperate broadleaf deciduous forests
VV	Vertical polarization transmit and vertical polarization receive
X-band	8 to 12 GHz electromagnetic spectrum frequency range

## List of symbols

$B$	Interferometric baseline
$B_n$	Perpendicular baseline
$s_x$	Complex image value
$R$	Range from satellite to target
$h_v$	Volume height
$z_0$	Ground topography
$\theta_B$	Look angle
$\theta_i$	Incidence angle
$H$	Orbit height
$h$	ALS-measured forest height
$\gamma$	Complex interferometric coherence
$\gamma_{Vol}$	Interferometric coherence volume decorrelation
$\gamma_{Temp}$	Interferometric coherence temporal decorrelation
$\gamma_{SNR}$	Additive noise decorrelation
$\gamma_{Sys}$	Decorrelation related to quantization errors
$\sigma_v$	Mean extinction coefficient
$k_z$	Vertical wavenumber
$\theta_0$	Interferometric incidence angle
$\lambda$	Wavelength
$\tilde{\gamma}_m$	Modelled complex interferometric coherence
$\vec{w}$	Polarization
$m$	Ground-to-volume amplitude ratio
$\tilde{\gamma}_V$	Modelled volume-only complex coherence
$\phi$	Interferometric phase on the ground
$\sigma$	Extinction parameter
$r^2$	Correlation coefficient
$std$	Standard deviation

# 1. INTRODUCTION

## 1.1. Background

Forest is one of the Earth's most significant natural resources and an integral part of national and global economies. The importance of forests in supporting life on Earth is distinctly reflected in the growing interest in international conservation and sustainable management of forests. Rising awareness of the challenges in retaining the health of this vital ecosystem is boosting conservation of biodiversity and accelerating the exploitation of new technologies. As modern remote sensing by satellites has matured, the field has made significant contributions to the monitoring of the atmosphere and biosphere on a planetary scale. Of particular interest to this research is the near continuous, high revisit monitoring of the global carbon cycle and of the state of forests worldwide.

Forests currently cover close to 4 billion hectares (ha) of land while suffering under a deforestation rate of 13 million hectares per year [1]. As one of the most diverse ecosystems on the planet, forest biomes cover 31% of the total land area [2] and hold approximately 80% of terrestrial above ground biomass [3]. Carbon accounts for roughly 50% of the dry weight of biomass [4]. However, the contribution of forestry-related carbon flux to global climate change is still difficult to forecast with confidence. Despite the efforts to aggregate the biomass estimates across different scales, the data acquisition and processing methodologies vary and cause uncertainties about the size and location of the terrestrial carbon sources and sinks [5, 6, 7].

The United Nations Framework Convention on Climate Change (UNFCCC) considers forest above ground biomass (AGB) as an essential climate variable [8] that plays a large role in the global carbon dynamics, in the forecasting of climate change and in its proposed mitigation strategies [9]. Approximately half of the carbon contained in forest vegetation and soil is located at high latitudes, where boreal and temperate forests are most extensive [10]. In Northern Europe, forestry is a dominant land use and wooded areas constitute the largest land cover type, accounting for 41% of the total land area in the European Union countries [11]. This alone sets forest and land cover related changes in Europe as the single largest source of carbon flux [12]. The temperate and boreal forests in the Northern Hemisphere act as a substantial carbon sink, while the carbon balance in those forests is largely controlled by anthropogenic activities [13].

Moreover, out-dated or missing data introduces further biases in the terrestrial carbon budget and climate change forecasting models [14]. Information about the state of forest resources and the economic damage caused by the disturbances are commonly acquired through field measurements or airborne photography and laser scanning [15, 16]. These methods can be efficiently used for mapping on a smaller scale, but prove insufficient when frequent up-to-date information and nation- or continent-wide surveys are needed, resulting in trade-offs

between cost, scale and accuracy of the measurements [17]. In addition, airborne laser surveys can be costly and aerial photography, similarly to optical satellite data, is influenced by cloud cover and lack of solar illumination.

Forest biome is sensitive to a variety of disturbances, including legal and illegal logging activity, deforestation, storm and fire damage and pest outbreaks. Despite numerous satellites in orbit, the Food and Agriculture Organization of the United Nations (FAO) has reported that at a global level there are still large data gaps concerning forest fires and illegal logging [2]. Some countries also suffer under the severe damage caused by insect pest-induced diseases and natural disasters which also remain largely underreported [2]. The estimates of the distribution of this major reserve for terrestrial carbon could be potentially fine-tuned through increased sustainable management of forests [18] and systematic integration of Earth Observation (EO) data with high quality ground measurements. The rapidly expanding number of EO satellites and advanced remote sensing techniques improve the coverage and consistency of the global dataset by allowing high-revisit and cost-effective monitoring of a wide range of forest and land cover parameters [19]. Field measurements are commonly used to accompany the remotely sensed data for calibration, extrapolation and validation of the dynamic vegetation cover models [20]. The major benefits of using space-borne sensors include filling of gaps in global data, updating and harmonizing of quality and other parameters of national inventory datasets [21], reducing errors in out-dated datasets [22, 23] and improving the mapping of yearly productivity and carbon sequestration by the vegetation [24].

EO satellites have been orbiting the Earth since 1960 [25] and continue a rapid increase in numbers with the addition of public and private satellites and satellite constellations. The EO community has seen the addition of optical, radar and other types of satellites for developing a number of vegetation remote sensing applications. The Landsat program paved the way as the longest continuous global spectral data provider since the early 1970s [26]. The first Earth-orbiting Synthetic Aperture Radar (SAR), Seasat, was launched in 1978, significantly increasing the remote sensing community's interest in imaging radars [27]. From 1991, the European Space Agency contributed to the global monitoring of land, water, ice and atmosphere with the successful European Remote Sensing Satellite ERS-1, followed by ERS-2 in 1995 and by ASAR on Envisat in 2002, to guarantee the continuity of the data stream for the environmental studies [28]. The launch of public-domain high resolution optical and radar imagery with global coverage, high revisit times and long-term observational commitment have further stimulated the growth in implementation of satellite data by public authorities and the private sector in Europe [29]. The best examples of this are the European Copernicus programme's Sentinel-1 and Sentinel-2 missions, launched in 2014 and in 2015 respectively, whose freely available datasets are used for a wide range of operational services.

Radar remote sensing satellites have opened up unique possibilities for mapping and monitoring vegetation from space on a daily basis, while offering a considerable variety and selection of different wavelength, coverage and

resolution options. Such data is needed on a regular basis to map deforestation and land conversion [30, 31], detect logging events [32, 33] and assess storm and fire damage [34, 35]. Global biomass estimates from radar satellites at continental scales provide an essential input for calculating carbon flux and monitoring changes in carbon stocks [36, 37].

Forest mapping from space relies mainly on optical remote sensing [38], imaging radar [39] and space-borne LiDAR (Light Detection And Ranging) scanning [40]. The advantages of microwave radar imaging compared to optical imaging for forestry applications are principally its sensitivity to the dielectric and geometrical properties of the targets, penetration capacity and coherent imaging properties [41]. SAR satellites are therefore capable of retrieving additional information, such as structure of the forest, tree height and growing stock volume (GSV) while working in nearly all weather conditions, independently of daylight and cloud cover [42]. Nevertheless, optical, LiDAR and radar imagery provide most benefits when used complementarily in developing forest remote sensing applications [43, 44].

Forest biomass, the key parameter for assessing the extent of forest resources worldwide [45], can be retrieved using the direct interpretation of the radar backscatter signal [46,47] or from tree height using allometric relations [48]. Many studies have demonstrated the successful use of SAR backscatter intensity measurements for forest biomass estimation using longer L-band (~27 cm) and P-band (~70 cm) wavelengths [49, 50, 51, 52, 53] in boreal [54, 55] and tropical forests [56, 57]. Despite the tendency to saturate with increasing stem volume [58], higher frequencies such as C-band SAR have also been proven to work well when using a large multi-temporal image stack, the best example being the forest biomass map of entire Northern Hemisphere [59]. The European Space Agency (ESA) has selected the Biomass SAR satellite mission operating in P-band as their next Earth Explorer, to emphasize the need for accurate and frequent global biomass maps of tropical, temperate and boreal forests [60, 7]. Also radargrammetry, a technique that can potentially be applied for wide-area boreal forest AGB mapping, is researched for operational use, but requires an additional accurate Digital terrain model (DTM) as a reference [61, 62, 63], which is not widely and regularly available.

The allometric relation between forest height and biomass has potential to increase the accuracy of biomass estimation even further as vegetation height mapping from X-band SAR data has shown promising results in producing accurate forest height estimations [48, 64, 65]. Forest height can be used as a variable for a number of environmental applications as it strongly correlates to several other forest properties, such as AGB [48, 66, 67, 68], forest age and density [56, 69] and can indicate changes in the forest [70]. Changes in forest height can also indicate problems with forest growth, diseases, natural disasters or human influence. In addition, accurately estimated forest height is valuable information for industry, in terms of timber production, biomass fuel potential or land parcel quality assessment and evaluation.

Information about the height, extent and coverage of the vegetation can be applied for practical applications such as updating forest cadastral data and sustainable forest management. Commercial applications that need high spatio-temporal coverage of vegetated areas include vegetation management of power line corridors and landscape modelling for efficient and profitable wind turbine location planning. For agricultural use, vegetation height can give valuable information about grassland cutting practices and demonstrate the effect of environmental conditions on crop growth cycle [71, 72].

The need for large-scale and cost-effective forest height measurements has in recent years resulted in strong interest in the Interferometric SAR (InSAR) data. The sensitivity of the interferometric measurements to forest vertical structure and the distribution of vegetation makes the technique valuable for improving forest resource monitoring [73, 74]. InSAR technique relies on coherently collected amplitude and phase signals, used for studying the phase differences between two complex-valued SAR images [75, 76]. Moreover, the coherence information, which is a measurement of phase stability or correlation between two simultaneously acquired radar images [41], is thus a valuable method for determining boreal [48, 64], tropical [77, 78, 79] and mangrove [80] forest height and biomass.

The traditionally used airborne Light Detection And Ranging (LiDAR) technique enables the direct measurement of forest height, whereas InSAR relies on exploiting model-based inversions for vegetation height estimation [81]. Interferometric coherence can be related to spatial variability of vegetation height through physics-based [82] or empirical relationships. The majority of InSAR forest height applications rely on multiple polarisation complex coherence images and require either fully polarimetric or dual-polarimetric InSAR data [65, 83]. Single-polarization measurements from space-borne SAR sensors could also provide accurate results when used together with auxiliary data such as digital terrain model (DTM) for determining the ground phase or other generalised assumptions about the ground scattering contribution and forest extinction parameters [65, 77, 83, 84]. In addition, airborne radar measurements have provided the opportunity to acquire data with different wavelengths and several antennas simultaneously, offering multiple polarizations and high spatial resolution [84]. Recent advancements in advanced remote sensing techniques, such as polarimetric interferometric SAR (PolInSAR), a concept first demonstrated in 1997, allows insight into extraction of different scattering mechanisms [85]. The separation of different types of scattering in turn allows forest classification of heterogeneous forests for enhanced detection of the tree species, structure, height, and biomass density [86].

For height estimation from interferometric coherence with short wavelength radar (e.g. C-band or X-band), the image pair acquisition should be done simultaneously or with a very short temporal baseline, insuring the minimal effect or absence of temporal de-correlation caused by the scatterers' displacement or changes in dielectric constant in between the two data takes. If the movements of leaves and branches caused by wind are eliminated, only volume decorrelation

is left which is dependent on forest height and can be effectively used for its estimation by interferometric coherence analysis [48]. Currently the only close formation tandem SAR satellite pair in orbit to provide simultaneous and global data acquisitions is the DLR (German Aerospace Center) mission TanDEM-X (TerraSAR-X add-on for Digital Elevation Measurement), operational since 2010 [87]. This single-pass radar interferometer carries out bistatic observations based on the two radar satellites flying in close formation and is thus not influenced by the effects of temporal decorrelation [87]. Although the principal mission objective is to create a three-dimensional map of the Earth's surface, it has opened up diverse opportunities for a number of other applications, e.g. bistatic InSAR coherence measurements which include the volume decorrelation can be related to the forest height [65].

Relating forest parameters to TanDEM-X single-polarized InSAR coherence can be achieved by applying physical models or supervised semi-empirical and empirical methods [21, 68, 88, 89, 90, 91]. Common methods are InSAR coherence magnitude based [48, 68, 89] and phase-based approaches combined with an external DTM [21, 90, 91]. However, there are currently no operational services that use space-borne interferometric SAR data for forest height estimation due to the complexity of the modelling, environmental variability and also the consistency in the measurement accuracy compared to the *in situ* or LiDAR data. Nevertheless, the scientific community is making significant steps closer for retrieving forest structure from space-borne imaging radars and developing sophisticated algorithms and models.

A number of studies have shown promising results with model-based methods for forest height retrieval in boreal [64, 67, 83, 92] and tropical [65, 77, 80] sites. The majority of the studies are carried out over relatively small test sites and use in-situ auxiliary data, which are not practical for large-scale applications. The dependence of operational, model-based forest height estimation algorithms on external data should be reduced to a minimum to avoid input data with varying quality and availability. Simple models based on the availability of single-polarized interferometric coherence data could be a good starting point for robust and universal applications.

The accuracy of height extraction from InSAR data is influenced by the forest related parameters such as extinction and contribution of ground scattering, which impact the coherence dynamics and vary depending on the imaging geometry and forest structure. Simplified inversion approaches allow data interpretation without the need for scarcely available fully polarimetric multi-parameter measurements and a large number of unknown model variables. The robust approach described in [93, 94, 95, 96] is based on single-polarized interferometric coherence data and simple semi-empirical models that do not need additional *a priori* parameters. The described approach holds a strong potential for the development of feasible operational canopy height retrieval application. The proposed coherence models are capable of describing the dynamics of InSAR coherence magnitude observed over hemiboreal forests and perform equally well for forest height retrieval in coniferous and deciduous

forests [95, 96]. Research on this topic is of significant interest to a number of scientific groups and efforts are made to develop the first operational accurate forest height maps from space, which allow forest stand height derivation up to an accuracy of a few meters. The main challenge lies in developing reliable and robust models for comprehensive forest height inversion in varying seasonal and environmental conditions.

## 1.2. Thesis objectives and progress of this work

The objective of this thesis is to assess the impact of different variables affecting hemiboreal forest height estimation from space-borne X-band interferometric SAR coherence data. The work concentrates on assessing changes in coherence dynamics related to seasonal conditions, tree species and imaging properties using a large collection of interferometric SAR images from different seasons over a four-year period.

The research was carried out using interferometric coherence magnitude, and aimed to demonstrate that similar height retrieval results can be achieved compared to commonly used phase-based approaches combined with external DTM or multi-polarimetric data, and to introduce simple models that can describe the forest height based on the availability of single-polarized interferometric coherence data. Applying several models and analysing the coherence dynamics over a large number of SAR images allowed the identification of the optimal conditions for hemiboreal forest height retrieval.

Several studies were carried out over large hemiboreal forested sites in Estonia, using an extensive dataset of single-polarized interferometric SAR images to observe the relation between the interferometric SAR coherence magnitude and the forest parameters under variable conditions. The studies concentrate on describing the data acquired over different seasons and environmental conditions, the impact of seasonal changes on the coherence dynamics and the stability of coherence magnitude data for wide area forest mapping.

The aim of the first study [I] was to assess the correlation of single-pass X-band SAR coherence magnitude and forest height using simple volume decorrelation analysis. The work demonstrates how the correlation of interferometric coherence and ALS-derived forest height varies for pine and deciduous tree species, for summer (leaf-on) and early spring (leaf-off) conditions and for flooded forest floor. However, there were notable deviations in the results caused by the temporal changes in the vegetation. Simple semi-empirical models were introduced to address the limitations of the regression model and to reduce the dependence of the height estimation accuracy on the imaging configuration and unknown empirical constants.

To improve the understanding of the seasonal effects on the interferometric SAR data, the number of TanDEM-X images on the Soomaa test site was increased to cover all seasons [II]. The impact by the different imaging parameters were considered during the implementation of the simple semi-empirical

model, derived from Random Volume over Ground model. Using the above-mentioned model, which contain one unknown parameter, it was possible to demonstrate the performance of forest stand height derivation during different seasons without *a priori* knowledge and remove the unknown empirical constants that are needed for regression model. The results of this study indicated that stable weather conditions and the use of a simple semi-empirical model allows to describe the coherence dynamics related to the height of coniferous and deciduous forests over all seasons. The most favourable conditions were found during low temperatures in winter when the relationship between coherence and forest height is easier to interpret than during summer conditions.

The suitability of different model-based approaches for forest height extraction from InSAR data were assessed to address these different inversion scenarios [III]. The study was extended to cover over 2200 ha of forests and over 3000 forest stands that were analysed using the multi-temporal set of 19 TanDEM-X interferometric image pairs. This is one of the largest datasets of SAR images from different seasons to be published for assessing the correlation between coherence magnitude and forest height. Models with different complexity levels were compared over boreal and deciduous forests in Estonia to demonstrate simpler mathematical models for describing the relationship between forest height and interferometric coherence. It was found that a simple semi-empirical modelling approach is capable of successfully describing the dynamics of InSAR coherence observed over hemiboreal forest, and is suitable for several forest types and for different seasonal conditions.

Further study [IV] focused on developing tools for hemiboreal forest height estimation from single-polarized interferometric SAR measurements and introducing height relative to the height of ambiguity as a parameter in the model fitting. The performance of the proposed four coherence models was analysed for three main forest types over all seasons in the hemiboreal zone.

It is one of the first scientific studies [IV] to demonstrate that the best argument for empirical models when relating coherence and forest parameters is the height relative to height of ambiguity (HoA), which should be used as a parameter in the model fitting. It was shown that all three models (linear, *sinc*-function, RVoG) provide a good fit with the measurements and have potential for forest height retrieval from space-borne interferometric X-band SAR while requiring only one fitting parameter. Different behaviour for winter and summer images was observed, with the frozen condition providing a good fit with the models and generally being the most favourable condition for model inversion. This study established the basis for the simple semi-empirical modelling approach that allows successful description of the dynamics of InSAR coherence observed over hemiboreal forests. The results of the research make use of the only currently available database of bistatic space-borne SAR images and could be used for future forest height estimation applications over wide forested areas.

## 2. INTERFEROMETRIC COHERENCE FOR FOREST HEIGHT RETRIEVAL

### 2.1. Radar scattering mechanisms in forest

The scattering of the radar signal is determined by the properties of the target, mainly by the surface roughness and dielectric properties of the medium, and by radar system imaging parameters, such as the wavelength, incidence angle and polarization. These imaging parameters determine how the wave interacts with canopies of different size and shape. Longer L-band (~27 cm) and P-band (~70 cm) wavelengths interact in the canopy primarily with the branches and the tree trunk as these scatterers have dimensions roughly in the same order with the wavelength. Shorter X-band (~3 cm) wavelengths interact with tree elements that have similar or larger dimensions and is therefore backscattered mostly from leaves, twigs, needles and smaller branches. This randomly distributed multiple scattering from foliage, defined as volume scattering, demonstrates the microwave radar sensitivity to the structure of the forest and the vertical distribution of the effective scatterers in the resolution cell [85].

Branches, leaves and tree trunks result in multiple scattering between elements and act as attenuators [27]. Different scattering mechanisms can be utilized with the polarimetric interferometric SAR (PolInSAR) technique by separating the effective phase centres of different scattering mechanisms to retrieve the parameters of the vertical structure of the forest [85]. In sparse forest, the signal is less attenuated and can reach the forest floor, resulting in a more significant ground reflection contribution. This effect can become even more significant in deciduous forests, during the leaf-off period. Studies with the X-band signal have demonstrated that penetration to the mixed deciduous forest during leaf-off period increases contribution from the trunk-ground interaction and the scattering from the flooded forest floor has a strong impact even for the short wavelength signal return [99, 100].

The environmental parameters that contribute to the backscattering from the canopy are mainly related to the water content in the canopy which has strong effect on the dielectric properties of the object. Therefore, the leaf water content and possible coverage with water drops affects the crown contribution to total backscatter [101]. The moisture parameters in a tree are determined by the content of liquid water that depends on the availability of water from the soil, seasonal conditions (snow cover) and also on the temperature [102]. With high leaf water content, the direct crown scattering contribution dominates and with low leaf water content the ground reflection and trunk scattering terms become more significant [101]. Freezing conditions can decrease the amount of liquid water in a tree and reduce the attenuation of the SAR signal in the canopy [103]. Even at temperatures of  $-15^{\circ}\text{C}$ , more than 25% of the water in the wood cell wall of different tree species has been found to be liquid, making it potentially transportable at temperatures well below  $0^{\circ}\text{C}$  [104]. Dry or frozen

conditions therefore allow deeper penetration of the SAR signal in the canopy and as a consequence weather conditions are important to consider when analysing the extinction of the microwave in the random volume [103, 105, 106].

The penetration depth and rate of attenuation in the canopy is mainly affected by the amount of moisture present, but varies also with different tree species and depends on the presence of understory layers [103]. Leaf-off and dry period in deciduous forests allows radar beam to penetrate deeper into the vegetation as it is less attenuated by the leaves [92, 107]. The ground surface of a forest is a horizontally oriented scatterer and results in a different polarimetric response compared to a volume scatterer such as randomly oriented forest canopy cover [108]. Therefore, the choice of transmit and receive polarization of the scattered waves can influence forest height estimation when using single-polarized data as the VV polarization has been found more suitable for flooded forest floors and wet conditions due to lower ground scattering contribution compared to HH polarization as demonstrated in Publication I and II and in [99, 100, 109].

## 2.2. Interferometric SAR measurements of forests

SAR Interferometry (InSAR) is a well-established and powerful radar remote sensing technique for generating high-resolution topographic maps and retrieving ground displacement information. Interferometry is based on the coherent combination of two radar images, allowing the retrieval of additional information by exploiting the phase differences of the SAR signals [75].

Depending on the application, the images are acquired under slightly different orbit positions or from the same orbit position but at different times. Simultaneous image acquisition from two different look angles is especially beneficial for forest height estimation purposes as it causes the interferometric coherence to decrease with increasing volume height due to the changes in the vertical scatterer arrangement [110]. The initial information about the forest volume and tree height can therefore be estimated from interferometric coherence as the random volume affects both interferometric phase and coherence. Additional properties such as penetration depth and the extinction of the radar wave in the medium can also be estimated from coherence [111].

Figure 2.1 shows a bistatic configuration of two SAR satellites (TerraSAR-X/TanDEM-X).

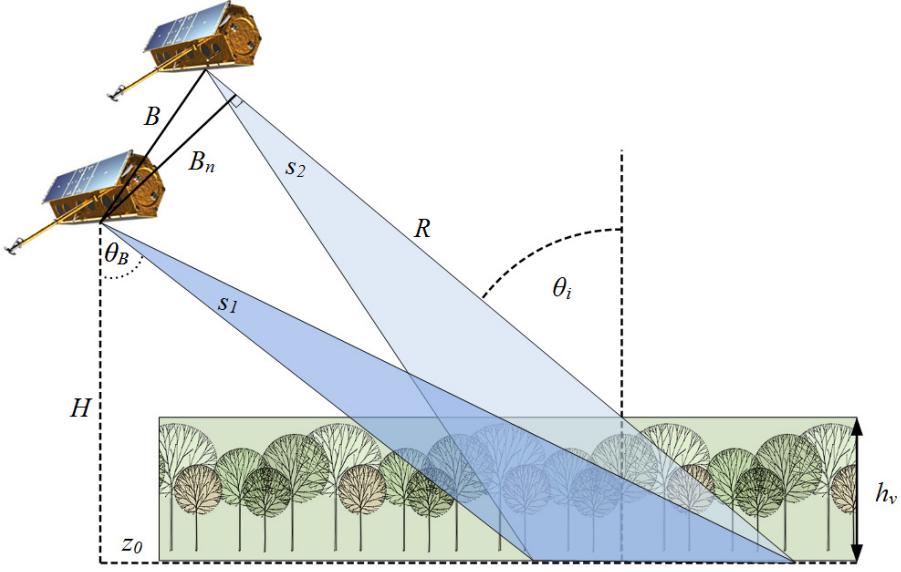


**Figure 2.1.** Bistatic configuration for across-track interferometry over forest canopy, where  $h_v$  is volume height,  $H$  is the satellite orbit height,  $z_0$  represents the ground topography,  $\theta_B$  is look angle and  $\theta_i$  is incidence angle. The two satellites are separated by the interferometric baseline  $B$  and the perpendicular baseline  $B_n$  to the line of sight. The corresponding signals  $s_1$  and  $s_2$  observe the object with the range to the target  $R$ .

The complex correlation coefficient, also known as interferometric coherence  $\gamma$ , is a measure of the degree of similarity between the two complex SAR measurements [85]. Coherence is defined as the normalized complex cross-correlation between the two signals,  $s_1$  and  $s_2$ :

$$\gamma = \frac{\langle s_1 s_2^* \rangle}{\sqrt{\langle s_1 s_1^* \rangle \langle s_2 s_2^* \rangle}}, 0 \leq |\gamma| \leq 1 \quad (2.1)$$

where  $*$  denotes complex conjugation,  $|\dots|$  the magnitude of complex value and  $\langle \dots \rangle$  an average over the ensemble of pixels, typically selected by a sliding window of size (azimuth  $\times$  range) in a single look complex (SLC) image. The magnitude of the complex coherence, which ranges from 0 to 1, is proportional to scatterer randomness and related to phase noise [75]. Therefore, the estimation accuracy of the interferometric phase is directly related to the loss in coherence, where  $|\gamma| < 1$  occurs due to the decorrelation effects such as different orbits and baselines, thermal noise, volume scattering and temporal variations [86].

The reduced phase accuracy of the master and slave SAR images can be a result of several contributing factors and is commonly formulated as a composition of four dominating decorrelation processes [85, 112, 113, 114]:

$$\gamma = \gamma_{Vol} \cdot \gamma_{Temp} \cdot \gamma_{SNR} \cdot \gamma_{Sys} \quad (2.2)$$

where  $\gamma_{SNR}$  is coherence loss due to the signal-to-noise ratio (SNR) of the data, a measure of image quality and additive system noise,  $\gamma_{Vol}$  shows the volume decorrelation caused by the different distribution of the vertical scatterers in a resolution cell,  $\gamma_{Temp}$  stands for decorrelation caused by the changes in the observed target over time and  $\gamma_{Sys}$  describes coherence decrease caused by the measurement system quantization, ambiguities and the relative shift of the Doppler spectra and baseline [115]. Coherence  $\gamma$  can effectively be used for forest height estimation after the necessary corrections are carried out.

In this research, data were acquired using the TanDEM-X satellite pair that operates with one transmitting antenna and two receiving antennas [87]. Therefore, the temporal scene decorrelation can be neglected and  $\gamma_{Temp} = 1$  as the bistatic configuration of two antennas provides simultaneous measurements of the same scene [87, 116].

The additive noise decorrelation  $\gamma_{SNR}$  caused by the antenna pattern variations of the two interferometric channels can be calculated from the signal-to-noise ratio (SNR) as a ratio between the backscattering coefficient sigma nought  $\sigma^0$  and the corresponding noise equivalent sigma zero (NESZ) pattern [117]. According to [65] the mean noise decorrelation remains relatively small, around 0.95 for the HH channel and 0.93 for the VV channel.

The spectral decorrelation appears when the vertical distribution of scatterers inside the resolution cell changes and results in the so-called volume decorrelation  $\gamma_{Vol}$ . This is a result of different projection of the vertical components of the scatterers into the interferometric images and cannot be removed through spectral filtering [118]. Volume introduced decorrelation without the ground contribution can be mathematically expressed and modelled as [84, 110, 119]:

$$\tilde{\gamma}_V = \frac{\int_0^{h_v} \exp\left(\frac{2\sigma_v z'}{\cos\theta_0}\right) \exp(ik_z z') dz'}{\int_0^{h_v} \exp\left(\frac{2\sigma_v z'}{\cos\theta_0}\right) dz'} \quad (2.3)$$

where  $\sigma_v$  stands for the mean extinction coefficient of the random volume layer,  $k_z$  is the vertical wavenumber,  $\theta_0$  as the mean incidence angle between two satellites,  $z'$  the variable for vertical dimension and  $h_v$  thickness of the volume layer [84].

Volume decorrelation can be considered as the key parameter for forest height retrieval because of its direct sensitivity to distribution of vertical scatterers within the forest volume that the radar wave passes [108,120]. In the case of a non-zero effective baseline the interferometric images are acquired at different angles as depicted in Figure 2.1. Consequently, the pixels in the range direction correspond to different layers of forest, resulting in different

amplitude and phase of the resolution cell [121]. The greater the angular difference of the InSAR image pair, the more the forest layers corresponding to the pixels differ with each other. This is the main cause for baseline-dependent coherence loss in a semi-transparent medium. This relationship means that the volume decorrelation decreases the coherence [114].

Moreover,  $\gamma_{Vol}$  is dependent on the length of the baseline between two antennas and the varying incidence angles change the length of the radar signal path through the canopy (as demonstrated also in Figure 2.1). As a result, the signal will pass through different forest structures making  $\gamma_{Vol}$  a measure of decorrelation over vegetated areas. Increasing the perpendicular across-track baseline will improve the sensitivity of the radar interferometer to height differences and thus improves the vegetation classification [118], whereas a shorter baseline limits the sensitivity to forest height variation but results in a higher level of coherence [65]. Furthermore, there are additional limits such as the critical baseline length for which the two signals become completely decorrelated or when a large baseline leads to ambiguities (by integer multiples of  $2\pi$ ) in the phase-to-height conversion [118].

It has been demonstrated with success that even the short wavelength X-band (3.1 cm) SAR signal can penetrate the vegetation, although caution must be taken as the result may also be influenced by the density and moisture content of the volume layer [91, 109]. Forest height can be estimated using the interferometric SAR analysis, either based on the coherence magnitude [68, 89], phase combined with an external digital terrain model DTM [21, 90, 91] or their combinations [82].

Radar imaging geometry is described by the effective vertical interferometric wavenumber  $k_z$  and for a bistatic measurement can be approximated as a function of the radar wavelength  $\lambda$  and the incidence angle  $\theta_i$ :

$$k_z = \frac{2\pi\Delta\theta_i}{\lambda \sin \theta_i} \approx \frac{2B_n}{R \sin \theta_i} \quad (2.4)$$

where  $B_n$  is the effective perpendicular baseline to the line of sight,  $R$  stands for the range to the target and  $\Delta\theta_i$  is the angular separation of the acquisitions in the direction of the resolution cell [65]. The vertical wavenumber can also be expressed as the height of ambiguity (HoA). For the bistatic case the height of ambiguity is the height difference corresponding to a complete  $2\pi$  cycle of the interferometric phase and provides information about the phase-to-height sensitivity in the interferogram [116]. The height of ambiguity (HoA) of the interferometric image pair can be expressed as:

$$HoA = \frac{\lambda R \sin \theta_i}{2B_n} = \frac{2\pi}{k_z} \quad (2.5)$$

## 2.3. Modelling SAR coherence for forest

The relation between the InSAR coherence and forest height can be described using empirical or semi-empirical supervised methods. For example, promising results have been achieved using linear regression [68, 88, 89, 90], non-linear regression [89, 90, 91] and non-parametric models [21].

One commonly used approach for retrieving forest parameters is implementing the Random Volume over Ground model (RVoG) [48, 65, 83, 110, 121] which requires a multi-polarimetric dataset or an additional input parameter such as a Digital Elevation Model (DEM) for successful height inversion [122]. The majority of approaches to estimate forest height from interferometric SAR are based on using the phase centre height and coherence and require either multi-polarimetric data and/or an external DTM [65, 83, 103]. However, such data is not widely and consistently available. Furthermore, forest is a very complex medium and the characterization of the forest should be simplified for modelling purposes [123]. The lack of independent measurements and high non-linearity of the model create a further necessity to use simpler models for forest parameter inversion.

Recent works [64, 98] and Publications **I**, **II**, **III**, **IV** demonstrate that there is also the possibility to achieve similar height retrieval results by using simply interferometric coherence magnitude without the requirement for any additional parameters. Simpler models, derived from the RVoG model, provide effective inversion with physical background, making it advantageous over regression models, which require training data.

### 2.3.1. The Random Volume over Ground model

Retrieval of the physical parameters from the interferometric data requires a model, which is able to relate the randomly oriented vegetation layer and ground parameters to the measured parameters [119]. The Random Volume over Ground (RVoG) is a simple model for describing the homogenous randomly oriented layer over ground topography  $z_0$  and can be expressed by [119, 124, 125]:

$$\tilde{\gamma}_m(\vec{w}) = \exp(i\phi) \frac{\tilde{\gamma}_V + m(\vec{w})}{1 + m(\vec{w})} \quad (2.6)$$

where the modelled complex interferometric coherence  $\tilde{\gamma}_m$  is a function of polarization  $\vec{w}$ . The scattering model connects the effective ground-to-volume amplitude ratio  $m$ , the volume-only complex coherence  $\tilde{\gamma}_V$  and the ground topography related phase  $\phi$ .

Although the RVoG model allows deriving forest height directly from InSAR coherence, it also requires solving for four unknown parameters which in turn requires a minimum of two independent complex measurements. The

problem can be solved with fully polarimetric data or, in its absence, also with partially polarized data. However, dual-polarized or single-polarized data needs to be supported with auxiliary data or with assumptions about the forest attenuation properties [65, 83]. Some of the commonly used methods to assist the inversion are use of a digital terrain model (DTM) for locating the ground surface, determining phase centre height location or signal extinction in the canopy, or presuming there is no ground scattering contribution to the measurements [65, 77, 83, 84].

### 2.3.2. Simplified coherence models for forests

As described above, the interferometric coherence can be connected to forest height by using other key properties of the canopy layer by the RVoG model, which is a function of volume height, topographic phase, extinction coefficient and contribution of ground scattering [83]. However, the complexity of the RVoG model hinders its applicability for operational forest height estimation, hence regression or simplified RVoG models are more practical choices. Further reasoning is that the availability of multi-polarized data, which would be essential for the RVoG model inversion, is very limited and this gives the advantage to semi-empirical models that also work with single-polarized data.

The regression analysis lacks in physical background and contains totally unknown empirical constants, which is why the simplified semi-empirical models have an advantage in describing inversion in different height retrieval scenarios (Publication **IV**). Functions derived from the RVoG model include physical interpretation and have an advantage for different inversion scenarios due to their theoretical background. By introducing simple semi-empirical models, it is possible to make use of the currently available single-polarized bistatic TanDEM-X dataset and retain a sufficient number of parameters for model inversion.

A simple linear approximation for the coherence magnitude and height relation can be constructed when simplifying the RVoG model to the extreme (Publication **IV**). The linear model is often used as the first step to describe the relation between forest height and InSAR coherence. The linear relationship can be derived from the RVoG model (Eq. 2.6) and can be written as:

$$\gamma_l = e^{i\phi} e^{i\pi\frac{h}{HoA}} \left(1 - \frac{h}{HoA}\right) \quad (2.7)$$

where  $\phi$  is the interferometric phase on the ground,  $h$  stands for forest volume thickness (height) and  $HoA$  is the height of ambiguity. In Eq. 2.7 and in all semi-empirical models derived from the RVoG model the ALS-measured forest height  $h$  is referred to as being the same measure as the volume thickness  $h_v$  in the RVoG model (Eq. 2.6). As defined in [95],  $\frac{h}{HoA}$  is a relative height of the volume layer related to distance between the interferometric fringes (fringe-

height-normalized). As a dimensionless parameter, it sets up a comparable reference for volume induced coherence and allows use of the same function for describing measurements with different baselines.

However, linear models are often oversimplified for describing the site details and the interferometric SAR data. The interferometric coherence magnitude and tree height relationship can be described with a *sinc*-function, derived from the RVoG model, along with an assumption about the low attenuation and absence of the ground contribution. The *sinc* model can be derived when substituting the simplified volume decorrelation function (as shown in Publication **IV**) into the RVoG model (Eq. 2.6) and assuming zero ground contribution:

$$|\gamma_{sinc}| = \text{sinc}\left(\pi \frac{h}{HoA}\right) \quad (2.8)$$

This *sinc* model is useful for coherence magnitude based inversion as demonstrated in [83] and Publications **I**, **II**, **III** and **IV**. However, more complex models are more accurate as they take into account also the ground contribution and the signal extinction in the forest volume or when the inversion requires the interferometric phase.

The basic dependencies of the forest height from the interferometric coherence and imaging parameters can be described by introducing additional parameters for the derived simplifications of the RVoG model. The simplified semi-empirical models that were constructed using empirical parameters  $C_{lin}$ ,  $C_{sinc}$  and  $C_{0ext}$  for potential forest height retrieval in the framework of this research are:

$$|\gamma_{linear}| = 1 - \frac{h}{HoA} C_{lin} \quad (2.9)$$

$$|\gamma_{sinc}| = 0.95 \cdot \text{sinc}\left(C_{sinc} \pi \frac{h}{HoA}\right) \quad (2.10)$$

$$|\gamma_{0ext}| = \left[ \left(1 - e^{i2.4\pi \frac{h}{HoA}}\right) \frac{HoA}{h} \frac{i}{2.4\pi} - 1 \right] \frac{1}{C_{0ext}} + 0.95 \quad (2.11)$$

Here, the linear model (Eq. 2.9) is based on Eq 2.7, the *sinc* model comes from Eq. 2.8 and the  $\theta_{ext}$  (Eq. 2.11) model is a result of combining the RVoG model (Eq. 2.6) with volume scattering model simplification (Eq. 7 in Publication **IV**) where the extinction parameter  $\sigma$  approaches zero and the profile function (Eq. 2.3) is assumed to be constant instead of being exponential. An additional constant of 0.95 is added in the Eqs. 2.10 and 2.11. This value is based on the results of  $\theta_{ext}$  model fit to the entire dataset in Publication **IV** and allows adjusting the model shape to match the majority of the data. The various decorrelation sources that typically reduce the coherence maximum below 1 are the thermal noise and the non-overlapping spectra due to the differences in

incidence angles of the two TDX system satellites [65]. Moreover, these three models do not contain additional dependency on the baseline as the  $h/HoA$  argument is used.

The essential dependencies between the interferometric coherence, forest height and imaging properties can be characterized successfully with the simplified coherence models derived from the RVoG model. The derived semi-empirical models are useful considering that the fully polarimetric data and therefore the number of independent measurements is not always widely available. Moreover, the simplified models are a practical choice for describing the dynamics of InSAR coherence over large areas and possibly also for operational forest height estimation applications.

### **3. SEASONAL AND ENVIRONMENTAL EFFECTS IN FOREST HEIGHT ESTIMATION [Publications I and II]**

#### **3.1. Study area and data**

For operational applications it is crucial to assure the stability and performance of the height retrieval models under different seasonal and environmental conditions and with varying imaging geometry. Although it is known that the dielectric properties of the forest medium affect the way SAR microwaves penetrates the vegetation, the impact of weather conditions on the model-based inversion of forest height has been studied to a very limited extent. In addition, the influence of different tree species on canopy height estimation using interferometric coherence magnitude has received little attention in the available literature. This research gives the first insight into these questions by analysing an extensive dataset of 23 TanDEM-X images (Table 3.1), acquired over hemiboreal forests of Estonia. Accompanied with the Airborne Lidar Scanning (ALS) based forest height maps, 840 stands covering 2291 ha of forests were analysed over three test sites (Figure 3.1). Hemiboreal forests represent a transitional zone between the boreal coniferous and temperate broadleaved deciduous forest and cover most of Estonia, often being diverse in its structure and composition [126].

The TanDEM-X Coregistered Single look Slant range Complex (CoSSC) product was processed for coherence magnitude calculation and compared to the 90th percentile ( $P_{90}$ ) forest height maps derived from airborne LiDAR scanning. Forest stands were divided into three groups by the dominant tree species (pine, spruce, mixed deciduous) based on the information from the forest inventory database [126]. The data were analysed stand-wise using a stand border map [127] with statistics calculated for each stand. This was followed by the object-based comparison of corresponding mean coherence magnitude and mean ALS forest height (Figure 3.2). The data from the Rannu and Soomaa test sites were used for initial regression models, and the data from the Peipsiveere and Soomaa TanDEM-X images for comparing different coherence models and describing the dynamics of InSAR coherence observed over hemiboreal forests.

**Table 3.1.** TanDEM-X bistatic stripmap (SM) images over Soomaa and Peipsiveere test sites and spotlight (SL) images over Rannu test site.

ID	Test site	Date	Mean incidence angle (°)	Height of Ambiguity (m)	Temperature (C°)	Precipitation (mm)	Polarization	Orbit	Resolution ground azimuth/range (m)
1	Soomaa	29-Dec-2010	44.6	41.4	-6.8	0	HH	Ascending	3.30/2.52
2	Soomaa	01-Aug-2011	36.2	45.9	18.6	0	HH	Ascending	3.30/2.99
3	Soomaa	03-March-2012	23.4	44.7	0.9	0	HH/VV	Ascending	6.60/2.96
4	Soomaa	08-March-2012	34.8	66.2	-2.7	0	HH/VV	Ascending	6.60/2.06
5	Soomaa	14-March-2012	23.4	43.6	-0.4	0	HH/VV	Ascending	6.60/2.96
6	Soomaa	25-March-2012	23.4	43.9	0.9	9.9	HH/VV	Ascending	6.60/2.96
7	Soomaa	05-April-2012	23.4	16.2	4.6	0	HH/VV	Ascending	6.60/2.97
8	Soomaa	05-April-2012	18.2	41.8	-3.7	0	HH/VV	Descending	6.60/3.76
9	Soomaa	15-April-2012	45.2	30.8	10.8	0	HH	Ascending	3.30/2.49
10	Soomaa	02-May-2012	34.8	24.7	13.4	0	HH/VV	Ascending	6.60/2.06
11	Soomaa	18-May-2012	43.4	32.7	12.3	11	HH	Ascending	3.30/2.57
12	Soomaa	30-May-2012	23.4	18.5	9.1	20.6	HH/VV	Ascending	6.60/2.97
13	Soomaa	03-Oct-2012	34.8	33.7	10.2	0	HH/VV	Ascending	6.60/2.06
14	Soomaa	11-Nov-2012	23.3	19.7	5.1	0	HH/VV	Ascending	6.60/2.97
15	Soomaa	16-Nov-2012	34.8	31.8	5.5	0	HH/VV	Ascending	6.60/2.06
16	Peipsiveere	04-Jan-2011	44.6	41.6	-5.2	22	HH	Ascending	3.30/2.51
17	Peipsiveere	09-Sept-2011	36.2	48.2	13.7	0.8	HH	Ascending	3.30/2.99
18	Peipsiveere	30-March-2012	45.2	30.1	1.6	3.1	HH	Ascending	3.30/2.49
19	Peipsiveere	5-Nov-2012	43.4	33.6	2.7	12.6	HH	Ascending	3.30/2.57
20	Rannu	19-April-2013	39.9	64.8	13.1	0.5	HH	Ascending	1.80/3.20
21	Rannu	02-June-2013	39.9	47.2	26.4	0	HH	Ascending	1.80/3.20
22	Rannu	13-June-2013	39.9	46.9	21.9	0	HH	Ascending	1.80/3.20
23	Rannu	27-July-2013	39.9	59.5	21.0	0	HH	Ascending	1.80/3.20

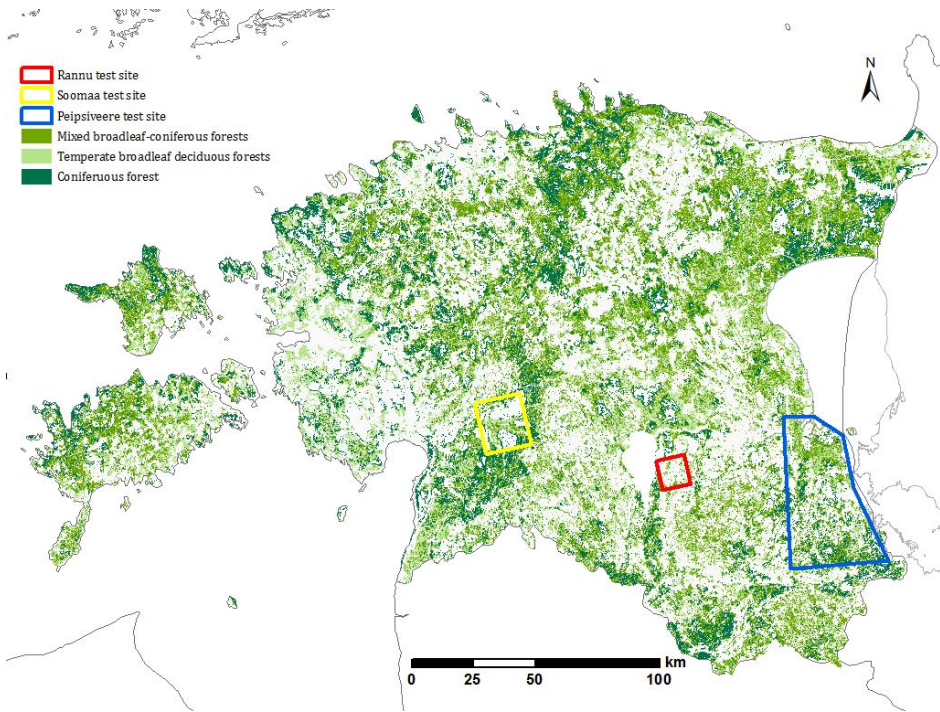


**Figure 3.1.** Locations of the Soomaa, Peipsiveere and Rannu test sites in southern Estonia. The map shows three forest classes according to the forest type.

## 3.2. Seasonal dynamics

### 3.2.1. Impact of temperature and water content changes on coherence

SAR systems are widely used for Earth Observation (EO) applications, in a large part due to their almost all-weather imaging capability. However, the water content influences the InSAR phase height in the vegetation as SAR is sensitive to total water amount and its distribution. Several studies have demonstrated that X-band SAR is subject to environmental influence such as precipitation, temperature change, frost and moisture [92, 103, 107] and that this variation should be included in the model analysis [66]. While wet conditions (rain, dew, melting snow) will increase the attenuation of the microwaves through the canopy, freezing does the opposite [103]. This effect was to some extent also observed in this research (Publications **I**, **II**, **III**, **IV**). Therefore, weather impact on the coherence data must be taken into account to ensure well-performing height retrieval models.

Besides the weather-induced influence on the signal penetration into the canopy [122], the deciduous trees result in higher temporal variations than coniferous forests due to the changing leaf-on and leaf-off conditions [65, 83,

92]. The large dataset of TanDEM-X images acquired over Estonia covers the climatic conditions throughout the year, providing the opportunity to analyse seasonal effects on coherence images.

During unvarying weather conditions, it has been found that the temporal stability of InSAR phase scattering centre height above the ground remains stable across summer to autumn images in coniferous forests [103, 128]. On the other hand, the sensitivity of SAR to water influences the signal penetration capabilities [65] and the wet condition can consequently introduce large variations. It was also observed in Publication IV that the differences in coherence dynamics were reduced during below-zero temperatures, when according to [103, 104], the majority of the liquid water is removed, resulting in deeper penetration of the microwave signals into the forest canopy. The example of this effect can be seen in Figure 3.2, where the winter image from 4 January 2011 (a) displays lower coherence compared to the autumn image from 9 September 2011 (c). As cold winter conditions seem to provide similar extinction properties and electrophysical parameters among similar forest types, it also allows to achieve better agreement with the coherence models.

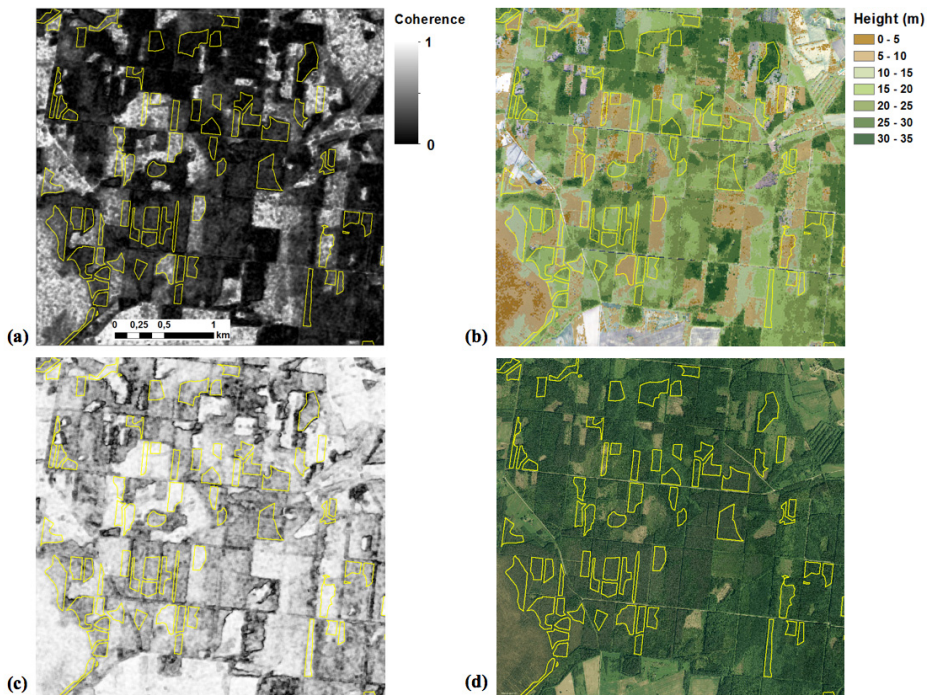


**Figure 3.2.** TanDEM-X coherence images from 4 Jan 2011 (a), taken with  $-5.2\text{ C}^\circ$  and 9 Sept 2011 (c), taken with  $-13.7\text{ C}^\circ$  are compared to corresponding LiDAR  $P_{90}$  forest height image from 29 June 2010 (b) and orthophoto (d) from 1 June 2011 [129]. The yellow polygons represent forest stands over a  $3.5 \times 3.5\text{ km}$  area, a subsection of Peipsiveere test site.

As also presented in Publication IV, below the freezing point temperatures on the day of the image acquisition (e.g. scenes from 04-Jan-2011, 03-Mar-2012, 08-Mar-2012, 14-Mar-2012, 25-Mar-2012) provide the best fit for coherence models as forest parameter estimation requires certain technical and preferably dry seasonal conditions, either frozen or unfrozen [103]. However, as proposed in Publication IV, the most favourable conditions for model inversion from single-polarized X-band data are achieved as a combination of HoA twice the height of the forest stand and below zero temperatures.

### 3.2.2. Effects of foliage seasonal variation on coherence

Correlation coefficients ( $r^2$ ) and standard deviations (std) were calculated for all the plots on the spring (leaf-off) and summer (leaf-on) images over Rannu test site and are presented in Publication I. Temporal variability of TanDEM-X interferometric measurements showed larger fluctuations in the standard deviation of deciduous trees during leaf-on period (Figure 3.3) ranging from 2.22 m to 3.16 m. During leaf-off period, the deciduous trees show a smaller deviation of 1.34 m to 1.78 m. It was found in Publication I that forest height estimation provides highest correlation coefficients for pine forests. However, when using a semi-empirical coherence model for fitting the data, the differences between the tree species and seasonal changes become minor.

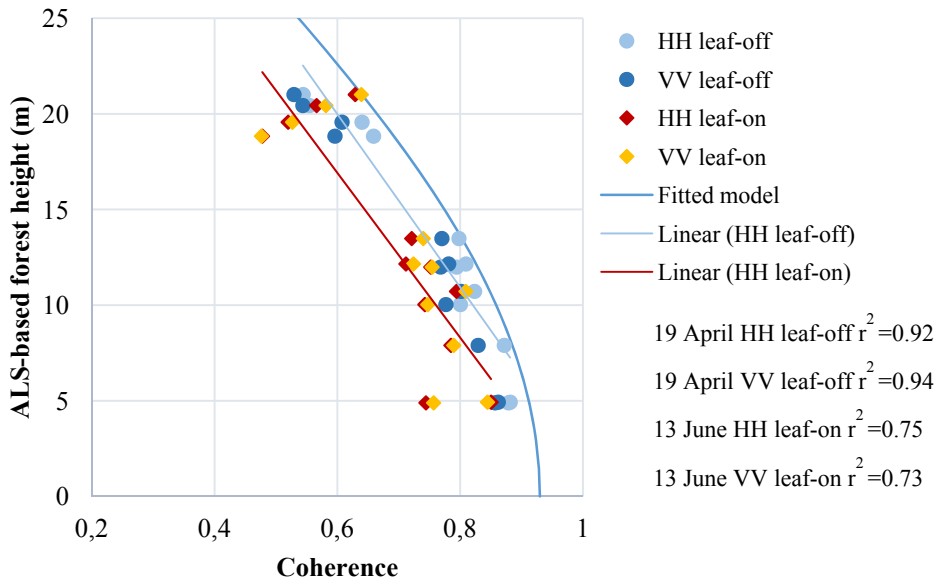


**Figure 3.3.** Comparison of mixed deciduous forests leaf-off conditions from 19 April 2013 (light and dark blue dots) and leaf-on conditions from 13 June 2013 (red and orange dots) on Rannu test site. The *sinc* (fitted) model shows best fit for the deciduous forests during leaf-off period.

### 3.2.3. Effect of flooded forest floors on coherence

Previous studies have demonstrated that flooded forest floors can strongly affect the SAR signal that penetrates the forests [130]. Even the short wavelength X-band SAR is sensitive to the water on the ground when the conditions are suitable, e.g. during leaf-off season in deciduous or mixed forests or over areas with lower and thinner forest canopy [99, 100].

Three images were acquired during leaf-off conditions in spring 2012 over Soomaa test site to study the effect of flooded forest floors on the coherence. Correlation coefficients ( $r^2$ ) and standard deviations (std) were calculated for the plots on the three images from March 2012. An increase in the standard deviation of deciduous plots was observed during the flooding of the rivers in the Pärnu River basin (Halliste, Raudna, and Lemmjõgi). The surrounding forested areas were flooded as a consequence of the river water level rising from 80 cm to 373 cm from the snowmelt water [131]. Standard deviation increased from 1.71 to 3.39 m in HH-polarized image while the change in VV-polarized image was only from 1.43 to 2.10 m, showing that X-band SAR signal can successfully penetrate the forest during leaf-off conditions and was, in this case, reflected from the ground. The VV polarization contained less ground scattering contribution compared to HH polarization as also noted in [109], particularly during leaf-off period and is therefore also less sensitive to floods. Consequently, wet and flooded forest floor conditions have smaller effect on the forest height estimation accuracy with the VV channel than the HH channel as shown in Publication I and in [99, 100], therefore VV polarization should mainly be considered for flooded environments as also demonstrated in Figure 3.4.

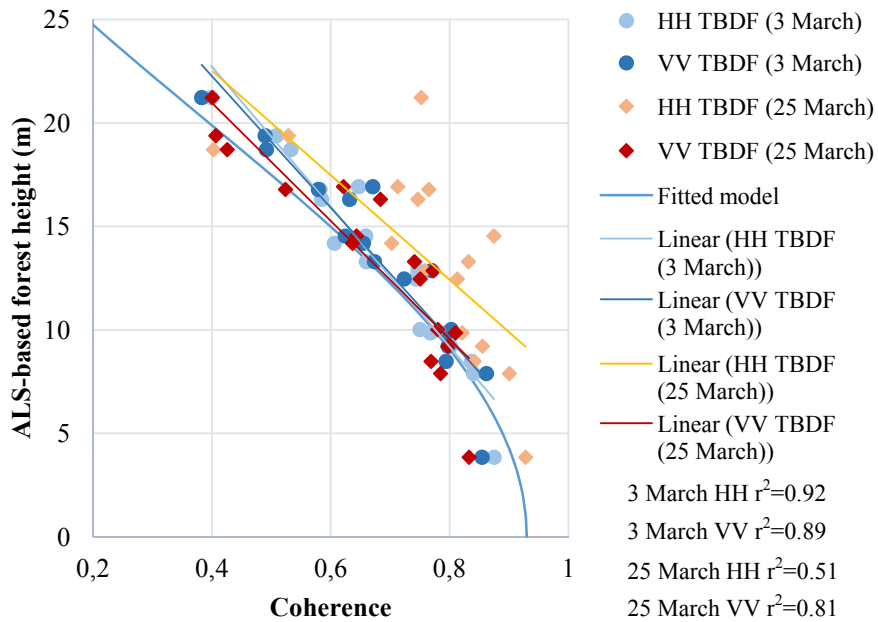


**Figure 3.4.** The *sinc* model shows a good alignment with the leaf-off temperate broadleaf deciduous forests (TBDF) on 3 March 2012 image, whereas the effect of flooding can be clearly seen on 25 March 2012 image. VV channel (red dots) contains less ground contribution than HH channel (orange dots) and results in higher correlation coefficient.

## 4. CHARACTERIZATION OF HEMIBOREAL FORESTS USING INSAR COHERENCE MODELS [Publications III and IV]

### 4.1. Stand height relative to Height of Ambiguity

The additional reliance of the linear, *sinc* and *0ext* model shapes on the baseline can be disregarded when considering the use of the  $h/HoA$  argument. Using  $h/HoA$  in the empirical models and plotting  $h/HoA$  values against the coherence magnitude will also reduce the impact of imaging configuration in relation to the actual forest height information. However, for the RVoG model  $h/HoA$  produces a different curve for every baseline, as the relation between the HoA and model shape is more complex.

The impact of the  $h/HoA$  argument on the relation between the coherence magnitude and ALS forest height is demonstrated in Figure 4.1 where 19 TanDEM-X (TDX) image pairs and 3787 forest stands have been analysed over different seasonal conditions, forest types and baseline configurations.

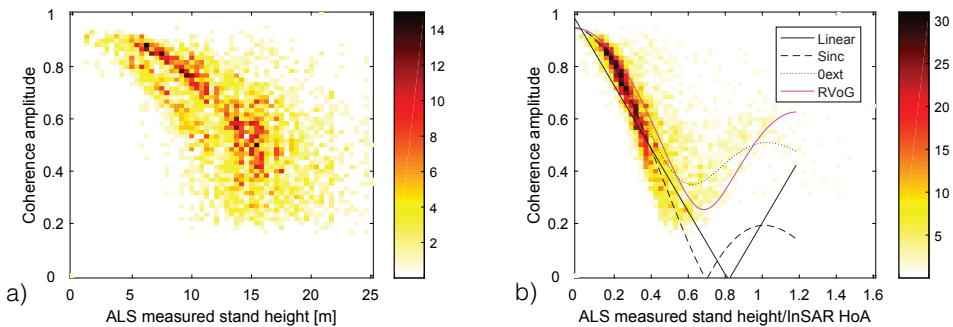


**Figure 4.1.** On the left (a) the TanDEM-X coherence amplitude is plotted against Airborne LiDAR Scanned (ALS) forest height for the 19 image pairs. On the right (b) the coherence magnitude is compared to ALS forest height divided by HoA (Eq. 2.5) values showing the benefit of using  $h/HoA$  as an argument. The colours represent how many coherence/stand height pairs fall into the value range (Publication IV).

### 4.2. Performance of the interferometric coherence models

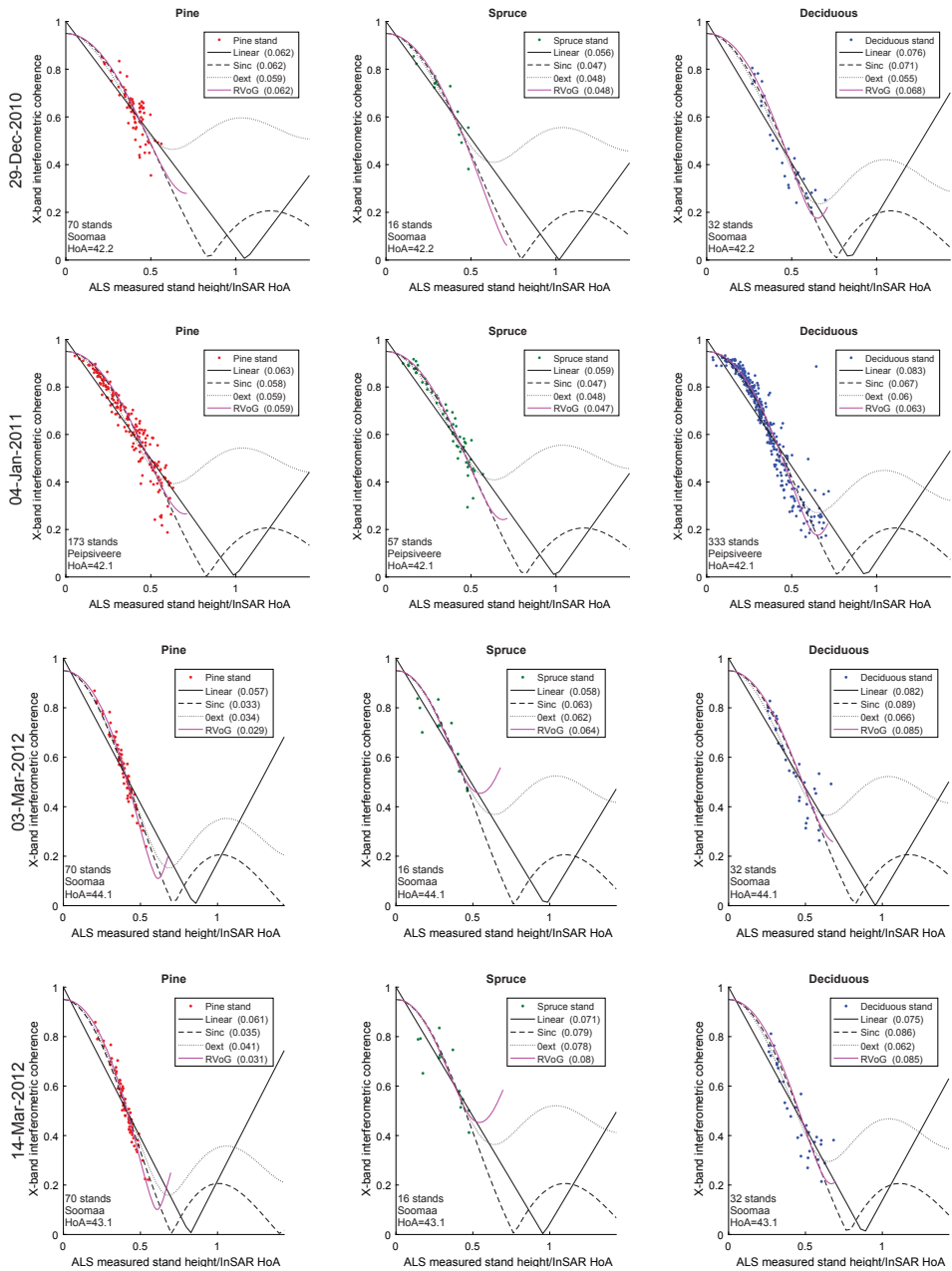
The proposed four coherence models (Eqs. 2.6, 2.9, 2.10, 2.11) were fitted to the individual interferometric scenes of hemiboreal forests acquired across a variety of seasonal and environmental conditions. A selection of the results is given as graphs in Figure 4.2, where the fit of four models across all stands and

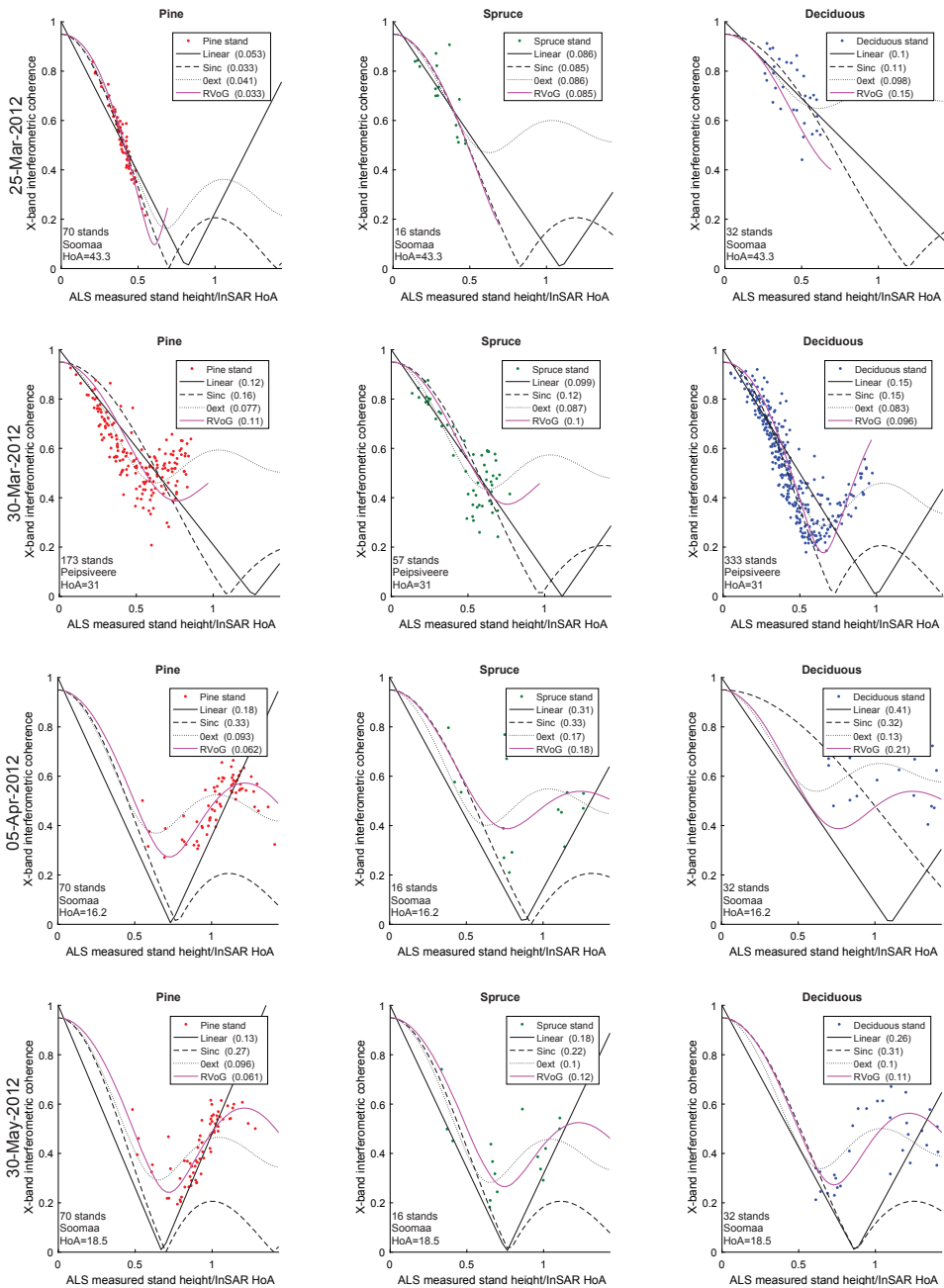
InSAR scenes is presented over the Soomaa and Peipsiveere test sites by using the ALS measured forest stand height as an argument.

It was found that in general, all forest scenes resulted in similar behaviour in respect to the measured coherence in  $h/HoA$  coordinates, particularly in the coherence range of 0.4–0.9. The scenes from 04-Jan-2011, 03-Mar-2012, 08-Mar-2012, 14-Mar-2012, 25-Mar-2012 showed even higher correlation, reaching the lowest section of the coherence values (0.2). In the low coherence areas, RVoG and  $\theta_{ext}$  model successfully described the variations in attenuation and ground reflection, whereas the *sinc* model showed less flexibility.

Moreover, the models result in similar fit for the  $h/HoA$  values larger than 0.2 and smaller than 0.6. The largest differences occur in the high coherence magnitude value area of  $>0.9$  where the linear model tends to perform inadequately. The best performance is provided by the  $\theta_{ext}$  and the RVoG models, while the linear model agrees well with the majority of the data except for the “tail” (coherence rising with increasing tree height starting at certain level) scenario and also for the very low ( $< 0.2$ ) and very high ( $> 0.9$ ) coherence magnitude values, which is also revealed in the graphs in Figure 4.2. Also, the *sinc* model is problematic in the region where stand height is close to the HoA.

In particular, the variations in the ground contribution tend to scatter the data and result in a “tail” scenario for the RVoG model. This is a result of the incapability of the model in describing the increase of coherence magnitude in response to the increasing  $h/HoA$  when reaching intermediate values (e.g. 30-March-2012 scene in Figure 4.2). Although the RVoG model adapts the best for a variety of cases, it can exhibit high sensitivity for smaller changes in coherence magnitude, which is not always favourable. The  $\theta_{ext}$  model has proven to be robust and can in certain conditions even outperform the RVoG model, e.g. in the low coherence region. Nevertheless, the RVoG model provides the best fit for the increasing coherence and  $h/HoA$  values, demonstrated in the 30-March-2012 scene in Figure 4.2. A single parameter model is preferred for large scale operational applications, where information about model parameters is likely to be absent.





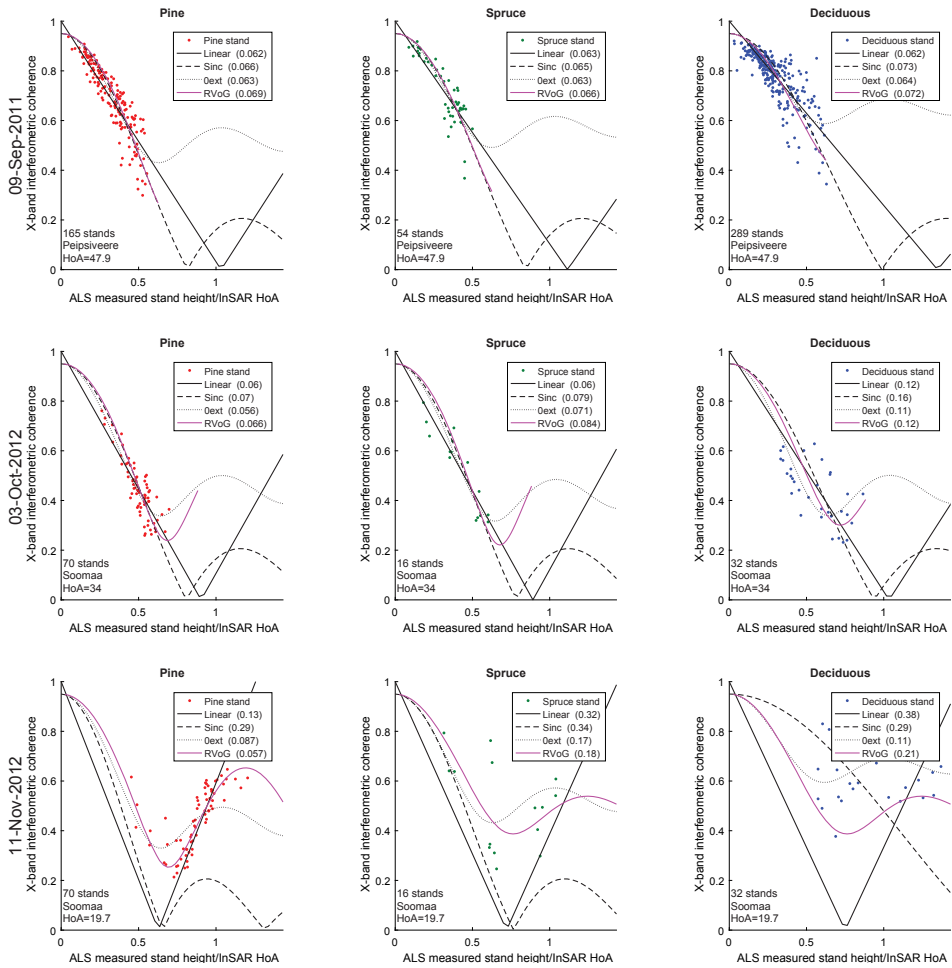


**Figure 4.2.** A selection of eleven different TanDEM-X InSAR scenes over the Soomaa and Peipsiveere test sites for showing the fit of four different models (Eqs. 2.6, 2.9, 2.10, 2.11) to coherence and ALS values for different tree species. The dominant tree species with the proportion >75% in the main tree layer are divided into pine stands (red), spruce stands (green) and deciduous stands (blue). Within the brackets is the goodness of fit parameter (RMSD).

### 4.3. Effect of tree species on the fit

Different tree species exhibit varying density and stratification properties and thus influence also the penetration, the extinction and the ground reflectivity values of the SAR signal. In Publication **IV** it was found that the dominant tree species have an observable effect on the model parameters, however, the differences between different scenes and acquisition dates are larger than the tree species-related differences. Overall, the differences between tree species were found to be small.

The best agreement with the models was achieved for the Scots pine stands with a possible explanation of the highest similarity between different stands on one scene. Furthermore, the smaller sample of spruce and deciduous dominated stands resulted in larger variability in most of the parameters.

The goodness of fit for four models over all forest stands and InSAR scenes is presented in Figure 4.3 and calculated as the root-mean-square deviation between the measured ( $x_i^{meas}$ ) and modelled ( $x_i$ ) coherence magnitude (Publication **IV**) for  $N$  number of examined stands:

$$RMSD = \sqrt{\frac{\sum_{i=1}^N (x_i - x_i^{meas})^2}{N}} \quad (4.1)$$

The darker bars represent the histograms for the scenes with HoA approximately twice as large as the highest stand height (04-Jan-2011, 03-Mar-2012, 08-Mar-2012, 14-Mar-2012, and 25-Mar-2012) and also demonstrate the positive outcome of the below zero weather conditions in winter scenes. Freezing conditions result in a more stable environment and thus a smaller variability in the SAR measurements, which also supports the previously made assumption of the similarity of attenuation properties.

Figure 4.3 demonstrates the improved performance by the  $\theta_{ext}$  and the RVoG models compared to the linear and  $sinc$  models, especially for the pine stands. Although linear model agrees well with most of the data, it lacks in describing the low coherence magnitude areas and also the very high coherence areas. Additionally, both linear and  $sinc$  models have problems with the increasing coherence magnitude in response to the increasing  $h/HoA$ , where the RVoG model outperforms all other models. The  $sinc$  model performs similarly to the linear model, while having the biggest difficulties describing the forest stands with heights close to the HoA values.

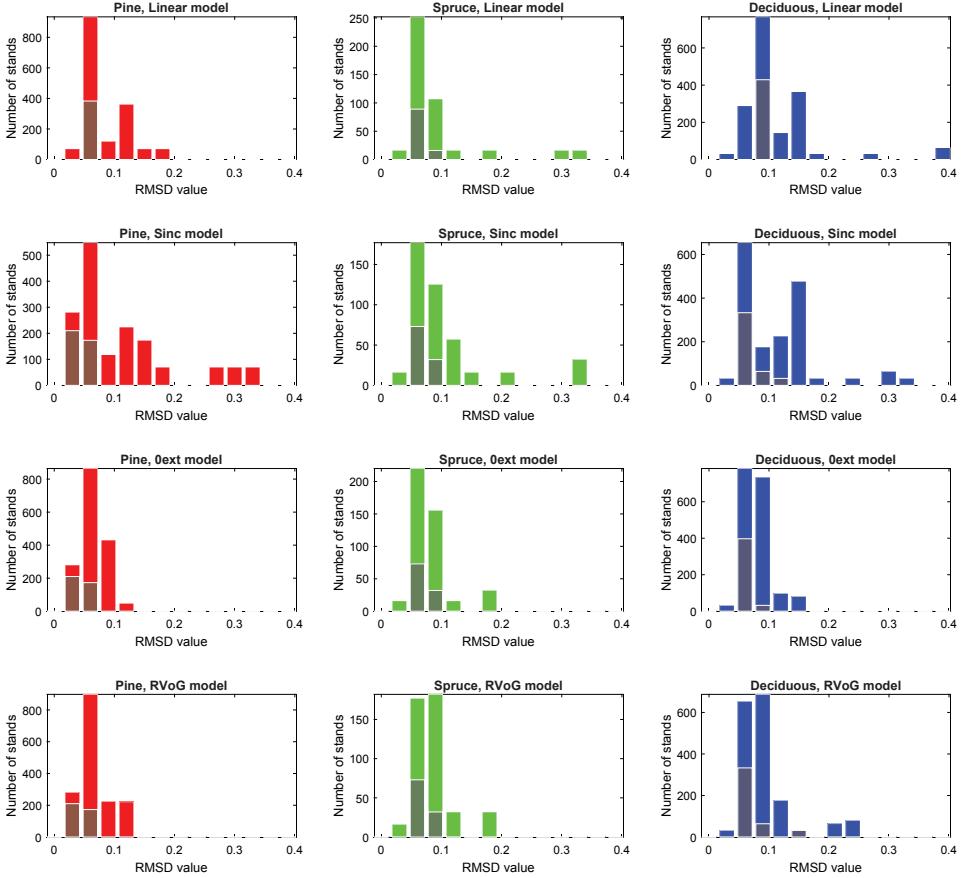


**Figure 4.3.** Goodness of fit for the linear, *sinc*, *Oext* and RVoG models (Eqs. 2.9, 2.10, 2.11, 2.6 respectively) for pine, spruce and deciduous forests. The Root Mean Square Difference (RMSD) is between the measured coherence magnitude and model predicted coherence (Publication IV).

#### 4.4. Model fitting dynamics related to the baseline

The performance of a coherence models and the goodness of fit is also influenced by the selection of the perpendicular baseline, which affects the vertical wave-number [65]. Figure 4.4 demonstrates the dependence of the coherence model RMSD on the height of ambiguity. The significance of the impact of HoA on the goodness of fit is particularly visible between the linear and *sinc* model fitting errors, mainly as a result of the poor adaption to the “tail” scenario. While the linear and *sinc* models cannot account for ground contribution and assume zero coherence on the ground, the RVoG and *Oext* model adapt well to variations in attenuation and ground reflection as demonstrated in Publication IV.

In addition to the visible impact of the HoA on the model agreement with the measurements, the scenes with HoA approximately twice the stand height are

set out as the most favourable for forest height inversion. Ideally, the HoA should be a compromise between different errors that are introduced with either too large or too small HoA values. HoA should be large enough to avoid height ambiguities and small enough to allow broad coherence dynamics. This is in line with observations in [103], where the optimal HoA for 30 m spruce forest is in the range of 20–50 m, allowing large coherence dynamics and trade-off between the errors.

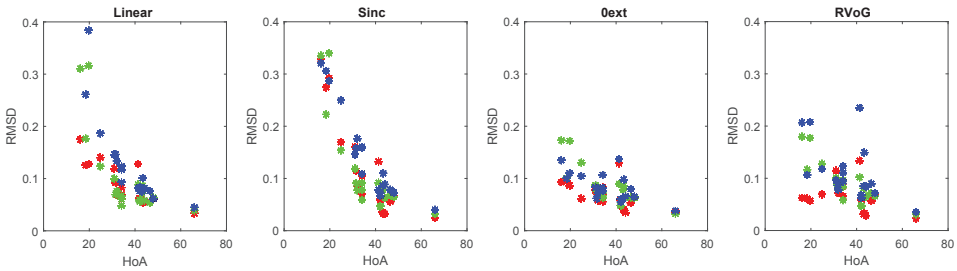


**Figure 4.4.** Dependence of the model fitting error on HoA for four different coherence models. Red asterisks stand for pine, green for spruce and blue for deciduous stands (Publication IV).

## 4.5. Comparison of the models

The four coherence models that were selected to describe the interferometric coherence magnitude of forest vegetation layer provide promising results for future forest height retrieval applications. Stable performance is achieved with each of the models over a variety of seasonal conditions and imaging properties, but with certain limitations. In addition, it was found that the models are suitable for describing both positive and negative correlation between the coherence magnitude and forest height. The “tail” scenario of the positive correlation is found in the area where the stand height was reaching the HoA values.

High coherence areas become a restraint to the single-parameter linear model, introducing biases. Furthermore, with the stand height close to the HoA, both linear and *sinc* model have difficulties in describing the low coherence areas. The slightly more complex two-parameter RVoG model allows to overcome some of the issues, but can introduce further complications in terms of invertability [84] and thus suitability for operational forest height estimation applications.

It was also found that the variations between the stands of the same dominant tree species on one image are smaller than the deviation between the same stands on different imaging dates. Furthermore, frozen conditions at the time of the image acquisition result in comparable electrophysical parameters and in turn allow to describe different forest stands by a single parameter defined empirical model curve. For operational applications, auxiliary data layers of the tree species should be integrated for increasing the reliability of the coherence models. Stable weather and environmental conditions, and HoA in the limits twice as large as expected maximal forest height, should be preferred.

## 5. CONCLUSION AND FUTURE WORK

This work investigates the applicability and performance of the space-borne interferometric X-band SAR coherence data for forest height retrieval over hemiboreal forests through assessment of the impact of seasonal conditions, tree species and imaging parameters on the interferometric coherence dynamics.

The studies were carried out over three test sites (Soomaa, Rannu and Peipsiveere) using the extensive multi-temporal dataset of 23 TanDEM-X images acquired over Estonia, covering 840 stands over 2291 hectares of forests. The bistatic single-pass coherence magnitude data was compared to Airborne Lidar Scanning (ALS)-measured forest stand heights for initial regression analysis and then compared with the coherence models. Correlation was found between interferometric coherence magnitude and ALS-measured forest stand heights across a variety of seasonal and environmental conditions, in deciduous and coniferous forests.

This study also provides insight into model fitting and describes the optimal conditions for large scale forest height retrieval. The Random Volume over Ground (RVoG) model and three semi-empirical coherence models were assessed for relating forest height to bistatic SAR coherence magnitude data and for assessing model performance under various conditions. The generally limited access to auxiliary forest data and, most importantly, fully polarimetric bistatic SAR data, restricts the applicability of the models on a global scale. As TanDEM-X is at present the only operational bistatic mission in space, applications are currently restricted to the routinely available single- or dual-polarized data. It was shown that applying the simple semi-empirical models provides the robustness of the height retrieval approach without the need for any additional reference data and *a priori* parameters.

The impact of temporal variability, imaging geometry and changing environmental conditions on the TanDEM-X interferometric measurements were investigated, along with the changes in the model dynamics for assessing the feasibility of the single-pass X-band bistatic SAR interferometric data for forest height retrieval. The preferable setting included dry conditions with below zero temperatures and a height of ambiguity of approximately twice the height of the forest stand height. The results confirm that given suitable and stable acquisition conditions and using fixed parameter values, there is potential for deriving forest stand height with an accuracy suitable for a wide range of applications. Simple models with suitable conditions demonstrated a feasible way for successful estimation of forest height or forest extinction properties via model inversion using single-polarized X-band data.

The potential of deriving large-scale forest height data using single-pass single-polarized interferometric space-borne X-band SAR coherence data was demonstrated using simple empirical and semi-empirical models. The simple linear model, *sinc* model, and zero extinction *0ext* model require only one fitting parameter and provide a simple and robust approach for describing the relation-

ship between forest height and interferometric coherence magnitude. Applying coherence magnitude and simplified RVoG models allowed assessment of the performance of forest height retrieval without the need for external digital terrain models or fully polarimetric SAR data. This approach holds a strong potential for feasible operational canopy height retrieval applications.

Future work could concentrate on developing applications for operational forest height retrieval, by demonstrating and applying forest height inversion based on the proposed semi-empirical models. This should allow for a fuller realisation of the potential of space-borne radar interferometer and for creating up-to-date, accurate and global forest height maps through simple and robust coherence models. In preparation for wide-area operational services, research could be carried out on using a grid-level approach instead of stand-level height retrieval. Furthermore, deriving forest above-ground biomass (AGB) from the InSAR coherence magnitude data using the species-specific allometric relations and biomass inversion models would provide important input to reducing the current uncertainties in global carbon dynamics.

## REFERENCES

- [1] FAO, *Global Forest Resources Assessment 2005: progress towards sustainable forest management (FRA 2005)*, FAO Forestry Paper 147, Food and Agriculture Organization of the United Nations, Rome, 2006.
- [2] FAO, *Global Forest Resources Assessment 2010: Main report*. FAO Forestry Paper 163, Food and Agriculture Organization of the United Nations, Rome, 2010.
- [3] F. S. Chapin III, P. A. Matson and P. Vitousek, *Principles of terrestrial ecosystem ecology*, Springer Science & Business Media, 2011.
- [4] R. A. Houghton, F. Hall and S. J. Goetz, “Importance of biomass in the global carbon cycle,” *Journal of Geophysical Research: Biogeosciences*, vol. 114, no. G2, 2009.
- [5] G. E. Kindermann, I. McCallum, S. Fritz and M. Obersteiner, “A global forest growing stock, biomass and carbon map based on FAO statistics,” *Silva Fennica*, vol. 42, no. 3, pp. 387–396, 2008.
- [6] R. A. Houghton, “Why are estimates of the terrestrial carbon balance so different?,” *Global change biology*, vol. 9, no. 4, pp.500–509, 2003.
- [7] ESA, *Report for Mission Selection: Biomass*, ESA SP-1324/1 (3 volume series), European Space Agency, Noordwijk, The Netherlands, 2012.
- [8] P. Mason and B. Reading, “Implementation plan for the global observing systems for climate in support of the UNFCCC,” In *Proceedings of the 21st international conference on interactive information processing systems for meteorology, oceanography, and hydrology*, San Diego, 2005.
- [9] FAO, *Assessment of the status of the development of the standards for terrestrial essential climate variables: Biomass (T12)*, Global Terrestrial Observing System, Rome, Italy, 2009.
- [10] R. K. Dixon, A. M. Solomon, S. Brown, R. A. Houghton, M. C. Trexier and J. Wisniewski, “Carbon pools and flux of global forest ecosystems,” *Science*, vol. 263, no. 5144, pp. 185–190, 1994.
- [11] Eurostat, “Land cover and land use, landscape (LUCAS),” [Online]. Available: [http://ec.europa.eu/eurostat/statistics-explained/index.php/Land\\_cover,\\_land\\_use\\_and\\_landscape#Further\\_Eurostat\\_information](http://ec.europa.eu/eurostat/statistics-explained/index.php/Land_cover,_land_use_and_landscape#Further_Eurostat_information) [Accessed 5 March 2015].
- [12] E. D. Schulze, P. Ciais, S. Luyssaert, M. Schrumppf, I. A. Janssens, B. Thiruchittampalam, J. Theloke, M. Saurat, S. Bringezu, J. Lelieveld, and A. Lohila, “The European Carbon and Greenhouse Gas Balance Revisited,” *Global Change Biology*, vol. 100, no. B, pp. 1451, 2010.
- [13] F. Magnani, M. Mencuccini, M. Borghetti, P. Berbigier, F. Berninger, S. Delzon, A. Grelle, P. Hari, P. G. Jarvis, P. Kolari and A. S. Kowalski, “The human footprint in the carbon cycle of temperate and boreal forests,” *Nature*, vol. 447, no. 7146, pp. 849–851, 2007.
- [14] Y. Pan, R. A. Birdsey, J. Fang, R. Houghton, P. E. Kauppi, W.A. Kurz, O. L. Phillips, A. Shvidenko, S. L. Lewis, J. G. Canadell and P. Ciais, “A large and persistent carbon sink in the world’s forests,” *Science*, vol. 333, no. 6045, pp. 988–993, 2011.
- [15] P. Gonzalez, G. P. Asner, J. J. Battles, M. A. Lefsky, K. M. Waring and M. Palace, “Forest carbon densities and uncertainties from Lidar, QuickBird, and field measurements in California,” *Remote Sensing of Environment*, vol. 114, no. 7, pp. 1561–1575, 2010.

- [16] L. Korhonen, K. T. Korhonen, M. Rautiainen and P. Stenberg, "Estimation of forest canopy cover: a comparison of field measurement techniques," *Silva Fennica*, vol. 40, no. 4, pp. 577, 2006.
- [17] S. Wertz-Kanounnikoff, L. V. Verchot, M. Kanninen and D. Murdiyarto, "How can we monitor, report and verify carbon emissions from forests?," In *Moving Ahead with REDD: Issues, Options and Implications*, Center for International Forestry Research (CIFOR), Bogor, Indonesia, 2008.
- [18] G. J. Nabuurs, O. Masera, K. Andrasko, P. Benitez-Ponce, R. Boer, M. Dutschke, E. Elsiddig, J. Ford-Robertson, P. Frumhoff, T. Karjalainen, O. Krankina, W. A. Kurz, M. Matsumoto, W. Oyhantcabal, N. H. Ravindranath, M. J. Sanz Sanchez and X. Zhang, "Forestry," In *Climate Change 2007: Mitigation. Contribution of Working Group III to the Fourth Assessment Report of the Intergovernmental Panel on Climate Change*, B. Metz, O.R. Davidson, P.R. Bosch, R. Dave, L.A. Meyer, eds., Cambridge University Press, Cambridge, United Kingdom and New York, NY, USA, 2007.
- [19] F. Achard and M. C. Hansen, eds., *Global forest monitoring from earth observation*. CRC Press, pp. 25, 2012.
- [20] S. J. Goetz, A. Baccini, N. T. Laporte, T. Johns, W. Walker, J. Kellndorfer, R. A. Houghton and M. Sun, "Mapping and monitoring carbon stocks with satellite observations: a comparison of methods," *Carbon balance and management*, vol. 4, no. 1, pp. 2, 2009.
- [21] K. Karila, M. Vastaranta, M. Karjalainen and S. Kaasalainen, "Tandem-X interferometry in the prediction of forest inventory attributes in managed boreal forests," *Remote Sensing of Environment*, vol. 159, pp. 259–268, 2015.
- [22] E. Tomppo, H. Olsson, G. Ståhl, M. Nilsson, O. Hagner and M. Katila, "Combining national forest inventory field plots and remote sensing data for forest databases," *Remote Sensing of Environment*, vol. 112, no. 5, pp. 1982–1999, 2008.
- [23] B. Koch, "Status and future of laser scanning, synthetic aperture radar and hyperspectral remote sensing data for forest biomass assessment," *ISPRS Journal of Photogrammetry and Remote Sensing*, vol. 65, no. 6, pp. 581–590, 2010.
- [24] T. Nilson, M. Rennel, A. Luhamaa, M. Hordo, A. Olesk and M. Lang, "MERIS GPP/NPP product for Estonia: I. Algorithm and preliminary results of simulation," *Forestry Studies*, vol. 56, no. 1, pp. 56–78, 2012.
- [25] J. B. Campbell and R. H. Wynne, *Introduction to remote sensing*, Guilford Press, 2011.
- [26] B. Ramachandran, C. O. Justice and M. J. Abrams, eds., *Land Remote Sensing and Global Environmental Change: NASA's Earth Observing System and the Science of ASTER and MODIS*. Springer Science & Business Media, vol. 11, pp. 4, 2010.
- [27] F. M. Henderson and A. J. Lewis, *Principles and applications of imaging radar. Manual of remote sensing, vol. 2*, John Wiley and sons, 1998.
- [28] Y. L. Desnos, H. Laur, P. Lim, P. Meisl and T. Gach, "The ENVISAT-1 Advanced Synthetic aperture radar processor and data products," In *Proceedings of the Geoscience and Remote Sensing Symposium (IGARSS'99)*, IEEE International, vol. 3, pp. 1683–1685, 1999.
- [29] M. Berger, J. Moreno, J. A. Johannessen, P. F. Levelt and R. F. Hanssen, "ESA's sentinel missions in support of Earth system science," *Remote Sensing of Environment*, vol. 120, pp. 84–90, 2012.

- [30] S. Quegan, T. Le Toan, J. J. Yu, F. Ribbes and N. Floury, “Multitemporal ERS SAR analysis applied to forest mapping,” *IEEE Transactions on Geoscience and Remote Sensing*, vol. 38, no. 2, pp. 741–753, 2000.
- [31] C. Thiel, P. Drezet, C. Weise, S. Quegan and C. Schmullius, “Radar remote sensing for the delineation of forest cover maps and the detection of deforestation,” *Forestry*, vol. 79, no. 5, pp. 589–597, 2006.
- [32] A. Olesk, K. Voormansik, M. Põhjala and M. Noorma, “Forest change detection from Sentinel-1 and ALOS-2 satellite images.” In *Proceedings of the 5th Asia-Pacific Conference on Synthetic Aperture Radar (APSAR)*, IEEE, pp. 522–527, 2015.
- [33] M. Santoro, J. E. S. Fransson, L. E. B. Eriksson and L. M. H. Ulander, “Clear-cut detection in Swedish boreal forest using multi-temporal ALOS PALSAR backscatter data,” *IEEE Journal of Selected Topics in Applied Earth Observations and Remote Sensing*, vol. 3, no. 4, pp. 618–631, 2010.
- [34] J. E. S. Fransson, A. Pantze, L. E. B. Eriksson, M. J. Soja and M. Santoro, “Mapping of wind-thrown forests using satellite SAR images,” In *Proceedings of the Geoscience and Remote Sensing Symposium (IGARSS)*, IEEE International, pp. 1242–1245, 2010.
- [35] S. Plank, “Rapid damage assessment by means of multi-temporal SAR – A comprehensive review and outlook to Sentinel-1,” *Remote Sensing*, vol. 6, no. 6, pp. 4870–4906, 2014.
- [36] T. Le Toan, S. Quegan, I. Woodward, M. Lomas, N. Delbart and G. Picard, “Relating radar remote sensing of biomass to modelling of forest carbon budgets,” *Climatic Change*, vol. 67, no. 2, pp. 379–402, 2004.
- [37] R. A. Houghton, “Aboveground forest biomass and the global carbon balance,” *Global Change Biology*, vol. 11, no. 6, pp. 945–958, 2005.
- [38] D. Lu, Q. Chen, G. Wang, L. Liu, G. Li and Emilio Moran, “A survey of remote sensing-based aboveground biomass estimation methods in forest ecosystems,” *International Journal of Digital Earth*, vol. 9, no. 1, pp. 63–105, 2016.
- [39] Sinha, S., C. Jeganathan, L. K. Sharma, and M. S. Nathawat. “A review of radar remote sensing for biomass estimation.” *International Journal of Environmental Science and Technology* 12, no. 5 (2015): 1779–1792.
- [40] E. T. A. Mitchard, S. S. Saatchi, A. Baccini, G. P. Asner, S. J. Goetz, N. L. Harris and S. Brown, “Uncertainty in the spatial distribution of tropical forest biomass: a comparison of pan-tropical maps,” *Carbon balance and management*, vol. 8, no. 1, 2013.
- [41] H. Maître, ed. *Processing of Synthetic Aperture Radar (SAR) Images*. John Wiley & Sons, 2013.
- [42] I. G. Cumming and F. H. Wong, *Digital processing of synthetic aperture radar data: algorithms and implementation*. Artech house, 2005.
- [43] S. Kaasalainen, M. Holopainen, M. Karjalainen, M. Vastaranta, V. Kankare, K. Karila and B. Osmanoglu, “Combining lidar and synthetic aperture radar data to estimate forest biomass: status and prospects,” *Forests*, vol. 6, no. 1, pp. 252–270, 2015.
- [44] O. Antropov, Y. Rauste, T. Hame and J. Praks, “Combining TanDEM-X and Landsat 8 data for improved mapping of forest biomass,” In *Proceedings of the Geoscience and Remote Sensing Symposium (IGARSS)*, IEEE International, pp. 3862–3865, 2015.

- [45] T. Le Toan, S. Quegan, M. W. J. Davidson, H. Balzter, P. Paillou, K. Papathanassiou, S. Plummer, F. Rocca, S. Saatchi, H. Shugart and L. Ulander, "The BIOMASS mission: Mapping global forest biomass to better understand the terrestrial carbon cycle," *Remote sensing of environment*, vol. 115, no. 11, pp. 2850–2860, 2011.
- [46] M. Santoro, C. Beer, O. Cartus, C. Schmullius, A. Shvidenko, I. McCallum, U. Wegmüller and A. Wiesmann, "Retrieval of growing stock volume in boreal forest using hyper-temporal series of Envisat ASAR ScanSAR backscatter measurements," *Remote Sensing of Environment*, vol. 115, no. 2, pp.490–507, 2011.
- [47] S. S. Saatchi, N. L. Harris, S. Brown, M. Lefsky, E. T. A. Mitchard, W. Salas, B. R. Zutta, W. Buermann, S. L. Lewis, S. Hagen and S. Petrova, "Benchmark map of forest carbon stocks in tropical regions across three continents," *Proceedings of the National Academy of Sciences*, vol. 108, no. 24, pp. 9899–9904, 2011.
- [48] A.T. Caicoya, F. Kugler, I. Hajnsek, and K. Papathanassiou, "Boreal forest biomass classification with TanDEM-X," In *Proceedings of the Geoscience and Remote Sensing Symposium (IGARSS)*, IEEE International, pp. 3439–3442, 2012.
- [49] T. Le Toan, A. Beaudoin, J. Riom and D. Guyon, "Relating forest biomass to SAR data," *IEEE Transactions on Geoscience and Remote Sensing*, vol. 30, no. 2, pp. 403–411, 1992.
- [50] A. Olesk, K. Voormansik, A. Luud, M. Rennel, K. Zalite, M. Noorma and A. Reinart, "Countrywide Forest Biomass Estimates From PALSAR L-Band Backscatter To Improve Greenhouse Gas Inventory In Estonia," In *Proceedings of the 6th Int. Workshop on Science and Applications of SAR Polarimetry and Polarimetric Interferometry (PolInSAR)*, L. Ouwehand, ESA Communications, ed., ESA SP-713, 128, ESA Publications Division, 2013.
- [51] M. Santoro, L. Ericsson, J. Askne, C. Schmullius, "Assessment of stand-wise stem volume retrieval in boreal forest from JERS-1 L-band SAR backscatter," *International Journal of Remote Sensing*, vol. 27, no. 16, pp. 3425–3454, 2006.
- [52] G. Sandberg, L. M. H. Ulander, J. E. S. Fransson, J. Holmgren and T. Le Toan, "L-and P-band backscatter intensity for biomass retrieval in hemiboreal forest," *Remote Sensing of Environment*, vol. 115, no. 11, pp. 2874–2886, 2011.
- [53] M. J. Soja, G. Sandberg and L. M. H. Ulander, "Regression-based retrieval of boreal forest biomass in sloping terrain using P-band SAR backscatter intensity data," *IEEE Transactions on Geoscience and Remote Sensing*, vol. 51, no. 5, pp. 2646–2665, 2013.
- [54] K. J. Ranson and G. Sun, "Mapping biomass of a northern forest using multi-frequency SAR data," *IEEE Transactions on Geoscience and Remote Sensing*, vol. 32, no. 2, pp. 388–396, 1994.
- [55] C. J. Thiel, C. Thiel and C. C. Schmullius, "Operational large-area forest monitoring in Siberia using ALOS PALSAR summer intensities and winter coherence," *IEEE Transactions on Geoscience and Remote Sensing*, vol. 47, no. 12, pp. 3993–4000, 2009.
- [56] A. Luckman, J. Baker, T. M. Kuplich, C. C. F. Yanasse and A. C. Frery, "A study of the relationship between radar backscatter and regenerating tropical forest biomass for spaceborne SAR instruments," *Remote Sensing of Environment*, vol. 60, no. 1, pp. 1–13, 1997.

- [57] S. Enghart, V. Keuck and F. Siegert, "Aboveground biomass retrieval in tropical forests – The potential of combined X-and L-band SAR data use," *Remote sensing of Environment*, vol. 115, no. 5, pp. 1260–1271, 2011.
- [58] M. Imhoff, "Radar backscatter and biomass saturation: ramifications for global biomass inventory," *IEEE Transactions on Geoscience and Remote Sensing*, vol. 33, no. 2, pp. 511–518, 1995.
- [59] M. Thurner, C. Beer, M. Santoro, N. Carvalhais, T. Wutzler, D. Schepaschenko, A. Shvidenko, E. Kompter, B. Ahrens, S. R. Levick, C. Schmullius, "Carbon stock and density of northern boreal and temperate forests," *Global Ecology and Biogeography*, vol. 23, no. 3, pp. 297–310, 2014.
- [60] S. Quegan and T. Le Toan, "Comparison of space-based technologies for measuring BIOMASS: The road to the BIOMASS mission," In *Proceedings of the Geoscience and Remote Sensing Symposium (IGARSS)*, IEEE International, pp. 7200–7203, 2012.
- [61] M. Vastaranta, M. Holopainen, M. Karjalainen, V. Kankare, J. Hyypä and S. Kaasalainen, "TerraSAR-X stereo radargrammetry and airborne scanning LiDAR height metrics in imputation of forest aboveground biomass and stem volume," *IEEE Transactions on Geoscience and Remote Sensing*, vol. 52, no. 2, pp. 1197–1204, 2014.
- [62] H. Persson and J. E. S. Fransson, "Forest variable estimation using radargrammetric processing of TerraSAR-X images in boreal forests," *Remote Sensing*, vol. 6, no. 3, pp. 2084–2107, 2014.
- [63] S. Solberg, G. Riegler and P. Nonin, "Estimating forest biomass from TerraSAR-X stripmap radargrammetry," *IEEE Transactions on Geoscience and Remote Sensing*, vol. 53, no. 1, pp. 154–161, 2015.
- [64] S. R. Cloude, H. Chen and D. G. Goodenough, "Forest Height Estimation and Validation Using Tandem-X Polinsar," In *Proceedings of the Geoscience and Remote Sensing Symposium (IGARSS)*, IEEE International, pp. 1889–1892, 2013.
- [65] F. Kugler, D. Schulze, I. Hajnsek, H. Pretzsch and K. P. Papathanassiou, "TanDEM-X PolInSAR Performance for Forest Height Estimation," *IEEE Transactions on Geoscience and Remote Sensing*, vol. 52, no.10, pp. 6404–6422, 2014.
- [66] J. I. H. Askne, J. E. S. Fransson, M. Santoro, M. J. Soja and L. M. H. Ulander, "Model-based biomass estimation of a hemi-boreal forest from multitemporal TanDEM-X acquisitions," *Remote Sensing*, vol. 5, no. 11, pp. 5574–5597, 2013.
- [67] J. Askne and M. Santoro, "On the Estimation of Boreal Forest Biomass From TanDEM-X Data Without Training Samples," *IEEE Geoscience Remote Sensing Letters*, vol. 12, no. 4, pp.771–775, 2015.
- [68] S. Abdullahi, F. Kugler and H. Pretzsch, "Prediction of stem volume in complex temperate forest stands using TanDEM-X SAR data," *Remote Sensing of Environment*, vol. 174, pp. 197–211, 2016.
- [69] M. J. Soja, H. Persson and L. M. H. Ulander, "Estimation of forest height and canopy density from a single InSAR correlation coefficient," *IEEE Geoscience and Remote Sensing Letters*, vol. 12, no. 3, pp. 646–650, 2015.
- [70] S. Solberg, E. Næsset, T. Gobakken and O. M. Bollandsås, "Forest biomass change estimated from height change in interferometric SAR height models," *Carbon balance and management*, vol. 9, no. 1, 2014.
- [71] K. Voormansik, T. Jagdhuber, A. Olesk, I. Hajnsek and K. P. Papathanassiou, "Towards a detection of grassland cutting practices with dual polarimetric

- TerraSAR-X data,” *International Journal of Remote Sensing*, vol. 34, no. 22, pp. 8081–8103, 2013.
- [72] K. Voormansik, T. Jagdhuber, K. Zalite, M. Noorma and I. Hajnsek, “Observations of cutting practices in agricultural grasslands using polarimetric SAR,” *IEEE Journal of Selected Topics in Applied Earth Observations and Remote Sensing*, vol. 9, no. 4, pp. 1382–1396, 2016.
- [73] R. Treuhaft and P. Siqueira, “The calculated performance of forest structure and biomass estimates from interferometric radar,” *Waves Random Media*, vol.14, pp. 345–358, 2004.
- [74] E. D. Wallington and I. H. Woodhouse, “Forest height retrieval from commercial X-band SAR products,” *IEEE Transactions on Geoscience and Remote Sensing*, vol. 44, no. 4, pp. 863–870, 2006.
- [75] R. Bamler and P. Hartl, “Synthetic aperture radar interferometry,” *Inverse problems*, vol. 14, no. 4, 1998.
- [76] D. Massonnet and J. C. Souyris, *Imaging with synthetic aperture radar*. CRC Press, 2008.
- [77] I. Hajnsek, F. Kugler, S. K. Lee and K. P. Papathanassiou, “Tropical-forest-parameter estimation by means of Pol-InSAR: The INDREX-II campaign,” *IEEE Transactions on Geoscience and Remote Sensing*, vol. 47, no. 2, pp. 481–493, 2009.
- [78] M. Schlund, F. von Poncet, D. H. Hoekman, S. Kuntz and C. Schmullius, “Importance of bistatic SAR features from TanDEM-X for forest mapping and monitoring,” *Remote Sensing of Environment*, vol. 151, pp. 16–26, 2014.
- [79] S. Solberg, T. P. Lohne and O. Karyanto, “Temporal stability of InSAR height in a tropical rainforest,” *Remote Sensing Letters*, vol. 6, no. 3, pp. 209–217, 2015.
- [80] S. K. Lee and T. E. Fatoyinbo, “TanDEM-X Pol-InSAR Inversion for Mangrove Canopy Height Estimation,” *IEEE Journal of Selected Topics in Applied Earth Observations and Remote Sensing*, vol. 8, no. 7, pp. 3608–3618, 2015.
- [81] T. Mette, K. Papathanassiou and I. Hajnsek, “Biomass estimation from polarimetric SAR interferometry over heterogeneous forest terrain,” In *Proceedings of the Geoscience and Remote Sensing Symposium (IGARSS)*, IEEE International, vol. 1, pp. 511–514, 2004.
- [82] S. Cloude, *Polarisation: applications in remote sensing*. Oxford University Press, 2010.
- [83] J. Praks, O. Antropov and M. T. Hallikainen, “LIDAR-aided SAR interferometry studies in boreal forest: Scattering phase center and extinction coefficient at X- and L-Band,” *IEEE Transactions on Geoscience and Remote Sensing*, vol. 50, no. 10, pp. 3831–3843, 2012.
- [84] J. Praks, F. Kugler, K. P. Papathanassiou, I. Hajnsek and M. Hallikainen, “Height estimation of boreal forest: Interferometric model-based inversion at L- and X-band versus HUTSCAT profiling scatterometer,” *IEEE Geoscience and Remote Sensing Letters*, vol. 4, no. 3, pp. 466–470, 2007.
- [85] S. R. Cloude and K. P. Papathanassiou, “Polarimetric SAR interferometry,” *IEEE Transactions on Geoscience and Remote Sensing*, vol. 36, no. 5, pp. 1551–1565, 1998.
- [86] J. S. Lee and E. Pottier, *Polarimetric radar imaging: from basics to applications, Optical Science and Engineering*. Taylor & Francis, Hoboken, NJ, 2009.
- [87] A. Moreira, G. Krieger, I. Hajnsek, D. Hounam, M. Werner, S. Riegger and E. Settelmeier, “TanDEM-X: a TerraSAR-X add-on satellite for single-pass SAR

- interferometry,” In *Proceedings of the Geoscience and Remote Sensing Symposium (IGARSS)*, IEEE International, vol. 2, pp. 1000–1003, 2004.
- [88] R. Treuhaft, F. Gonçalves, J. R. dos Santos, M. Keller, M. Palace, S. N. Madsen, F. Sullivan and P. M. L. A. Graça, “Tropical-forest biomass estimation at X-band from the spaceborne TanDEM-X interferometer,” *IEEE Geoscience and Remote Sensing Letters*, vol. 12, no. 2, pp. 239–243, 2015.
- [89] M. Schlund, F. von Poncet, S. Kuntz, C. Schullius and D. H. Hoekman, “TanDEM-X data for aboveground biomass retrieval in a tropical peat swamp forest,” *Remote Sensing of Environment*, vol. 158, pp. 255–266, 2015.
- [90] S. Solberg, R. Astrup, J. Breidenbach, B. Nilsen and D. Weydahl, “Monitoring spruce volume and biomass with InSAR data from TanDEM-X,” *Remote Sensing of Environment*, vol. 139, pp. 60–67, 2013.
- [91] S. Solberg, R. Astrup, T. Gobakken, E. Næsset and D. J. Weydahl, “Estimating spruce and pine biomass with interferometric X-band SAR,” *Remote Sensing of Environment*, vol. 114, no. 10, pp. 2353–2360, 2010.
- [92] J. Praks, M. Hallikainen, O. Antropov, and D. Molina, “Boreal forest tree height estimation from interferometric TanDEM-X images,” In *Proceedings of the Geoscience and Remote Sensing Symposium (IGARSS)*, IEEE International, pp. 1262–1265, 2012.
- [93] A. Olesk, K. Voormansik, A. Vain, M. Noorma and J. Praks, “Seasonal differences in forest height estimation from interferometric TanDEM-X coherence data,” *IEEE Journal of Selected Topics in Applied Earth Observations and Remote Sensing*, vol. 8, no. 12, pp. 5565–5572, 2015.
- [94] A. Olesk, K. Voormansik, T. Tamm, M. Noorma and J. Praks, “Seasonal effects on the estimation of height of boreal and deciduous forests from interferometric TanDEM-X coherence data,” In *Proceedings of the SPIE Remote Sensing*, International Society for Optics and Photonics, 26–29 September 2015, Toulouse, France, pp. 964406–964406, 2015.
- [95] A. Olesk, J. Praks, O. Antropov, T. Arumäe, K. Zalite and K. Voormansik, “Interferometric SAR Coherence Models for Characterization of Hemiboreal Forests using TanDEM-X Data,” *Remote Sensing*, vol. 8, pp. 700, 2016.
- [96] J. Praks, A. Olesk, K. Voormansik, O. Antropov, K. Zalite, M. Noorma, “Building blocks for semi-empirical models for forest parameter extraction from interferometric X-band SAR images,” In *Proceedings of the Geoscience and Remote Sensing Symposium (IGARSS)*, IEEE International, 10–15 July 2016, Beijing, China, pp. 736–739, 2016.
- [97] F. Kugler, S. K. Lee, I. Hajnsek and K. P. Papathanassiou, “Forest Height Estimation by Means of Pol-InSAR Data Inversion: The Role of the Vertical Wavenumber,” *IEEE Transactions on Geoscience and Remote Sensing*, vol. 53, no. 10, pp. 5294–5311, 2015.
- [98] H. Chen, D. G. Goodenough, S. R. Cloude and P. Padda, “Wide area forest height mapping using Tandem-X standard mode data,” In *Proceedings of the Geoscience and Remote Sensing Symposium (IGARSS)*, IEEE International, pp. 3782–3785, 2015.
- [99] K. Zalite, K. Voormansik, A. Olesk, M. Noorma and A. Reinart, “Effects of Inundated Vegetation on X-Band HH–VV Backscatter and Phase Difference,” *IEEE Journal of Selected Topics in Applied Earth Observations and Remote Sensing*, vol. 7, no. 4, pp. 1402–1406, 2014.

- [100] K. Voormansik, J. Praks, O. Antropov, J. Jagomagi and K. Zalite, "Flood Mapping with TerraSAR-X in Forested Regions in Estonia," *IEEE Journal of Selected Topics in Applied Earth Observations and Remote Sensing*, vol. 7, no. 2, pp. 562–577, 2014.
- [101] S. C. Steele-Dunne, J. Friesen and N. van de Giesen, "Using diurnal variation in backscatter to detect vegetation water stress," *IEEE Transactions on Geoscience and Remote Sensing*, vol. 50, no. 7, pp. 2618–2629, 2012.
- [102] S. S. Saatchi and M. Moghaddam, "Estimation of crown and stem water content and biomass of boreal forest using polarimetric SAR imagery," *IEEE Transactions on Geoscience and Remote Sensing*, vol. 38, no. 2, pp. 697–709, 2000.
- [103] S. Solberg, D. J. Weydahl and R. Astrup, "Temporal stability of X-band single-pass InSAR heights in a spruce forest: Effects of acquisition properties and season," *IEEE Transactions on Geoscience and Remote Sensing*, vol. 53, no. 3, pp. 1607–1614, 2015.
- [104] J. P. Sparks, G. S. Campbell and R. A. Black, "Liquid water content of wood tissue at temperatures below 0 C," *Canadian journal of forest research*, vol. 30, no. 4, pp. 624–630, 2000.
- [105] J. Way, J. Paris, E. Kasischke, C. Slaughter, L. Viereck, N. Christensen, M. C. Dobson, F. Ulaby, J. Richards, A. Milne and A. Sieber, "The effect of changing environmental conditions on microwave signatures of forest ecosystems: preliminary results of the March 1988 Alaskan aircraft SAR experiment," *International Journal of Remote Sensing*, vol. 11, no. 7, pp. 1119–1144, 1990.
- [106] C. Thiel and C. Schmullius, "Investigating the impact of freezing on the ALOS PALSAR InSAR phase over Siberian forests," *Remote Sensing Letters*, vol. 4, no. 9, pp. 900–909, 2013.
- [107] C. Demirpolat, "X-band interferometric radar for mapping temporal variability in forest," M.S. thesis, Aalto University, 2012.
- [108] R. N. Treuhaft and P. R. Siqueira, "Vertical structure of vegetated land surfaces from interferometric and polarimetric radar," *Radio Science*, vol. 35, no. 1, pp. 141–177, 2000.
- [109] F. Kugler and I. Hajnsek, "Forest characterisation by means of TerraSAR-X and TanDEM-X (polarimetric and) interferometric data," In *Proceedings of the Geoscience and Remote Sensing Symposium (IGARSS)*, IEEE International, pp. 2578–2581, 2011.
- [110] S. R. Cloude and K. P. Papathanassiou, "Three-stage inversion process for polarimetric SAR interferometry," *IEE Proceedings-Radar, Sonar and Navigation*, vol. 150, no. 3, pp. 125–134, 2003.
- [111] T. Mette, "Forest biomass estimation from polarimetric SAR interferometry," PhD diss., Technische Universität München, 2007.
- [112] E. Rodriguez and J.M. Martin, "Theory and design of interferometric synthetic aperture radars," *IEE Proceedings F-Radar and Signal Processing*, vol. 139, no. 2, pp. 147–159, 1992.
- [113] H.A. Zebker and J. Villasenor, "Decorrelation in interferometric radar echoes," *IEEE Transactions on Geoscience and Remote Sensing*, vol. 30, no. 5, pp. 950–959, 1992.
- [114] J. O. Hagberg, L. M. H. Ulander and J. Askne, "Repeat-pass SAR interferometry over forested terrain," *IEEE Transactions on Geoscience and Remote Sensing*, vol. 33, pp. 331–340, 1995.
- [115] G. Krieger, A. Moreira, H. Fiedler, I. Hajnsek, M. Werner, M. Younis and M. Zink, "TanDEM-X: A Satellite Formation for High-Resolution SAR Inter-

- ferometry,” *IEEE Transactions on Geoscience and Remote Sensing*, vol. 670, no. 45, pp. 3317–3341, 2007.
- [116] M. Martone, B. Bräutigam, P. Rizzoli, C. Gonzalez, M. Bachmann and G. Krieger, “Coherence evaluation of TanDEM-X interferometric data,” *ISPRS Journal of Photogrammetry and Remote Sensing*, vol. 73, pp. 21–29, 2012.
- [117] D. Just and R. Bamler, “Phase statistics of interferograms with applications to synthetic aperture radar,” *Applied optics*, vol. 33, no. 20, pp. 4361–4368, 1994.
- [118] G. Krieger, I. Hajnsek, K. P. Papathanassiou, M. Younis and A. Moreira, “Interferometric synthetic aperture radar (SAR) missions employing formation flying,” *Proceedings of the IEEE*, vol. 98, no. 5, pp. 816–843, 2010.
- [119] K. P. Papathanassiou and S. R. Cloude, “Single-baseline Polarimetric SAR Interferometry,” *IEEE Transactions on Geoscience and Remote Sensing*, vol. 39, no. 11, pp. 2352–2363, 2001.
- [120] M. Pardini, A. T. Caicoya, F. Kugler, S. K. Lee, I. Hajnsek and K. Papathanassiou, “On the estimation of forest vertical structure from multibaseline polarimetric SAR data,” In *Proceedings of the Geoscience and Remote Sensing Symposium (IGARSS)*, IEEE International, pp. 3443–3446, 2012.
- [121] R. N. Treuhaft, S. N. Madsen, M. Moghaddam and J. J. Van Zyl, “Vegetation characteristics and underlying topography from interferometric radar,” *Radio Science*, vol. 31, no. 6, pp. 1449–1485, 1996.
- [122] S. R. Cloude, POL-InSAR training course. Tutorial of the ESA Polarimetric SAR Processing (PolSARPro) Toolbox, 2008.
- [123] T. Le Toan, G. Picard, J. M. Martinez, P. Melon and M. Davidson, “On the relationships between radar measurements and forest structure and biomass,” In *Retrieval of Bio-and Geo-Physical Parameters from SAR Data for Land Applications*, vol. 475, pp. 3–12, 2002.
- [124] M. Brandfass, C. Hofmann, J. C. Mura and K. P. Papathanassiou, “Polarimetric SAR interferometry as applied to fully polarimetric rain forest data,” In *Proceedings of the Geoscience and Remote Sensing Symposium (IGARSS)*, IEEE International, vol. 6, pp. 2575–2577, 2001.
- [125] J. Praks “Radar polarimetry and interferometry for remote sensing of boreal forest.” PhD diss., Aalto University, Department of Radio Science and Engineering, 2012.
- [126] European Environment Agency (EEA), EEA Technical Report No9/2006, [Online]. Available: <http://www.env-edu.gr/Documents/European%20forest%20types.pdf> [Accessed on 26 August 2016].
- [127] Estonian Environment Agency (EEIC), [Online]. Available: <http://www.keskkonnaagentuur.ee/> [Accessed on 20 April 2016].
- [128] J. Praks, C. Demirpolat, O. Antropov and M. Hallikainen, “On forest height retrieval from spaceborne X-band interferometric SAR images under variable seasonal conditions,” In *Proceedings of the XXXII Finnish URSI Conv. Radio Sci. SMARAD Semin.*, Otaniemi, Finland, pp. 115–118, 2013.
- [129] Estonian Land Board Geoportal X-GIS Public Webmap Service, [Online]. Available: <http://xgis.maaamet.ee/xGIS/XGIS> [Accessed on 25 June 2016].
- [130] J. L. Place, “Mapping of forested wetland: Use of Seasat RADAR images to complement conventional sources,” *Professional Geographer*, vol. 37, no. 4, pp. 463–469, 1985.
- [131] Estonian Meteorological and Hydrological Station Weather Observations. [Online]. Available: <http://www.ilmateenistus.ee/?lang=en> [Accessed on 24 April 2016].

## SUMMARY

This thesis presents research in the field of radar remote sensing and contributes to the forest monitoring application development using space-borne synthetic aperture radar (SAR). Satellite data is particularly useful for large-scale forestry applications making high revisit monitoring of the state of forests worldwide possible. The sensitivity of SAR to the dielectric and geometrical properties of the targets, penetration capacity and coherent imaging properties make it a unique tool for mapping and monitoring forest biomes. SAR satellites are also capable of retrieving additional information about the structure of the forest, tree height and biomass estimates as an essential input for monitoring the changes in the carbon stocks.

Interferometric SAR (InSAR) is an advanced SAR imaging technique that allows the retrieval of forest parameters while working in nearly all weather conditions, independently of daylight and cloud cover. This research concentrates on assessing the impact of different variables affecting hemiboreal forest height estimation from space-borne X-band interferometric SAR coherence data. In particular, the research analyses the changes in coherence dynamics related to seasonal conditions, tree species and imaging properties using a large collection of interferometric SAR images from different seasons over a four-year period.

The study is carried out over three test sites in Estonia using the extensive multi-temporal dataset of 23 TanDEM-X images, covering 2291 hectares of forests to describe the relation between the interferometric SAR coherence magnitude and forest parameters. The work demonstrates how the correlation of interferometric coherence and Airborne LiDAR Scanning (ALS)-derived forest height varies for pine and deciduous tree species, for summer (leaf-on) and winter (leaf-off) conditions and for flooded forest floor. A simple semi-empirical modelling approach is proposed as being suitable for wide area forest mapping with limited a priori information under a range of seasonal and environmental conditions. A Random Volume over Ground (RVoG) model and three semi-empirical models are compared and validated against a large dataset of coherence magnitude and ALS-measured data over hemiboreal forests in Estonia.

The results show that all proposed models perform well in describing the relationship between hemiboreal forest height and interferometric coherence, allowing in future to derive forest stand height with an accuracy suitable for a wide range of applications.

# KOKKUVÕTE (SUMMARY IN ESTONIAN)

## Hemiboreaalsete metsade kaardistamine interferomeetrilise tehisava-radari andmetelt

Käesolev doktoritöö uurib tehisavaradari (SAR) kasutusvõimalusi metsa kõrguse hindamiseks hemiboreaalsete metsade vööndis. Uurimistöö viidi läbi Tartu Ülikooli, Tartu Observatooriumi, Aalto Ülikooli, Euroopa Kosmoseagentuuri (ESA) kaugseire keskuse ESRIN ja Reach-U koostöös. Uurimistöös kasutatud satelliidiandmed on pärit Saksa Kosmosekeskuse (DLR) kõrghälgutusega bistaatilise X-laineala tehisavaradari TanDEM-X satelliidipaarilt.

Sagedasti uuenevad satelliidiandmed, nende globaalne katvus ja kõrge ruumiline lahutus võimaldavad tehisavaradari abil kaardistada metsi ning nendes toimuvaid muutusi suurtel maa-aladel. Radari abil on võimalik saada kõrge lahutusvõimega pilte, mis on tundlikud taimestikule, maapinna karedusele ja dielektrilistele omadustele. Sünkroonis lendava radaripaari samaaegselt tehtud pildid elimineerivad võimalikud ajalised muutused taimestikus ning tänu sellele on radariandmetest võimalik tuletada metsade vertikaalset struktuuri ja kõrgust.

Uurimistöös käsitletakse tehisavaradari interferomeetrilise koherentsuse tundlikkust metsa kõrguse suhtes ning analüüsitakse, millised keskkonna ja kliimatilised tingimused ning satelliidi orbiidiga seotud parameetrid mõjutavad radari-piltidelt erinevate puuliikide kõrguse hindamise täpsust. Lisaks keskendub väitekirj interfeeromeetrilisele koherentsusele tuginevate mudelite analüüsimisele ning nende täpsuse hindamisele operatiivse metsa kõrguse kaardistamise rakenduseks. Vaatluse alla on võetud kolm testala, mis asuvad Soomaa rahvusparkis, Võrtsjärve idakaldal Rannus ja Peipsiveere looduskaitsealal ning katavad kokku 2291 hektarit metsa. 23 TanDEM-X satelliidipildi koherentsuspilte võrreldakse samadel testaladel aerolaserskaneerimise (LiDAR) abil mõõdetud puistute kõrgusega, mis on omakorda jagatud kolme rühma (kuused, männid ja laialehised segametsad).

RVoG (Random Volume over Ground) taimekatte mudel ning sellest tuletatud lihtsamad pooleempiirilised mudelid sobituvad olemasolevate TanDEM-X koherentsuse ning LiDARi metsa puistute kõrgusandmetega hästi. Töö tulemused kinnitavad, et tulevikus on suurte ja erinevatest metsatüüpidest koosnevate metsade kõrguse kosmosest kaardistamisel otstarbekas kasutusele võtta esmalt just soovitatud lihtsamad ja universaalsemad mudelid.

## ACKNOWLEDGEMENTS

There are many people who have played an important part in my research career. I am very grateful for their advice and help on many different matters, which have made this work possible. This thesis would not have been finalised without the kind support and collaboration with all the people acknowledged below.

I would like to thank my supervisors Mart Noorma, Kaupo Voormansik and Jaan Praks for their continuous support, inspiration and encouragement over these challenging years of PhD research. Mart has influenced many people, including me, with his passion and enthusiasm for space, often providing a welcome reminder of the significance of our research to human society when it is all too easy to get bogged down in research detail. I am very grateful to Kaupo who first introduced me to the world of radar remote sensing and invited me to be a part of the new young SAR research group. I highly appreciate the numerous discussions about SAR and Kaupo's patience in enlightening me on how to navigate within this complex research field. I am extremely grateful for the commitment and support by Jaan; his knowledge and experience in forest remote sensing has been invaluable for the progress of this research. Our frequent discussions on a wide range of research problems and publishing on the matter are greatly acknowledged.

I am grateful for Tiit Nilson for his support during the early days of my research career and collaboration in managing ESA R&D projects in Regio. I would also like to acknowledge Anu Reinart for giving me the opportunity to be part of the research community in the space research centre at Tartu Observatory and for supporting my traineeship in the European Space Agency.

I would also like to thank my colleague Karlis Zalite with whom I had the pleasure to share the PhD studies experience, collaborate on several articles and prepare for exams. I am grateful to Martin Valgur for his help with programming and solving technical obstacles. I have been honoured to be part of scientific discussions and collaborate with such talented co-authors and colleagues as Oleg Antropov, Tauri Arumäe, Tanel Tamm, Mait Lang and Ants Vain.

My special gratitude goes to my many ESRIN colleagues and particularly to Yves-Louis Desnos for supervising my traineeship in the European Space Agency Earth Observation centre at ESRIN. I feel very fortunate to have had the experience of spending a year working in ESA among Earth Observation specialists and space professionals and am thankful for their support, guidance and encouragement. I would also like to thank all the international trainees, especially Zina, Georgia, Georgiana and Marcela, who made the year in Italy unforgettable.

I would like to thank my friends, especially Õie, Liisi, Gerda, Helen and Brit who have always provided wonderful support and advice to keep me grounded during the five years of my PhD marathon.

I am thankful for all my friends and colleagues at Reach-U and Regio, especially Priit and Mattias, for supporting my journey and for accepting my double life with the university over the past five years. I am thankful for Teet Jagomägi for being my Reach-U supervisor under the DoRa scholarship of research cooperation between universities and businesses and making it possible to apply my research in Reach-U. The majority of this research has been funded by the Government of Estonia through an ESA Contract under the PECS (Plan for European Cooperating States) and I am very fortunate to have had the chance to lead these space projects in Reach-U.

My sincere gratitude goes to my always supportive parents Aime and Ahto who have helped me through the difficult times and made everything possible to help me to stay focused on my studies. My brother Arko has been a knowledgeable companion, with whom I have had many in depth discussions on the scientific world and our shared experiences as PhD students. I would like to thank Richard for his continuous support on my long journey, his patience and encouragement and consistent effort to perfect my English.

My research has been undertaken with the support of European Social Fund's Doctoral Studies and Internationalisation Programme DoRa, carried out by Foundation Archimedes. I gratefully merit the Archimedes Foundation for funding my PhD studies under DoRa scholarship EFS T3, the experience gaining in the European Space Agency under DoRa scholarship EFS T6 and also visits to several conferences under Kristjan Jaak Program.



## **PUBLICATIONS**

## ERRATA

### Publication I

On page 3, the Height of Ambiguity (HoA) values in Table 1 are incorrect. The correct values are:

Date	HoA (m)
3.03.2012	44.7
8.03.2012	66.2
25.03.2012	43.9
19.04.2013	64.8
2.06.2013	47.2
13.06.2013	46.9
27.07.2013	59.5

### Publication II

On page 964406, the Height of Ambiguity (HoA) values in the Table 1 are incorrect. The correct values are:

Date	HoA (m)
2010-12-29	41.4
2011-08-01	45.9
2012-03-03	44.7
2012-03-08	66.2
2012-03-14	43.6
2012-03-25	23.4
2012-04-05	16.2
2012-04-15	30.8
2012-05-02	24.7
2012-10-03	33.7
2012-11-16	31.8
2012-11-11	19.7

### Publication III

On page 738, the Eq. 7 should be:

$$\gamma_{0ext} = \left( [e^{ih2.4\pi/HoA} - 1] \frac{HoA}{h} \frac{1}{2.4\pi i} + C_5 \right) \frac{C_6}{1+C_5}$$

## CURRICULUM VITAE

**Name:** Aire Olesk  
**Date of birth:** 16 December 1985, Jõgeva, Estonia  
**Citizenship:** Estonian  
**Address:** Tartu Observatory, 61602, Tõravere, Estonia  
**Telephone:** +372 5220939  
**E-mail:** aire@ut.ee

**Education:**  
2012–2016 University of Tartu, PhD student  
2008–2011 University of New South Wales (Sydney, Australia), Surveying and Spatial Information Systems, MEng  
2005–2008 University of Tartu, Geography, BSc

**Professional career:**  
2011–... Reach-U, Technical project manager, remote sensing specialist  
2013–... Tartu Observatory, Junior Research Fellow  
2012–2013 European Space Agency (ESA-ESRIN), National Trainee – Stagiaire  
2008–2011 Sensis (Sydney, Australia), GIS Technician  
2006–2008 Regio, GIS Analyst

**Scholarships:**  
2015 Archimedes Foundation, Kristjan Jaak scholarship for foreign visits  
2013 Archimedes Foundation, Kristjan Jaak scholarship for foreign visits  
2012–2016 Archimedes Foundation, DoRa scholarship EFS T3 – Activity 3 – Strengthening research cooperation between universities and businesses  
2012 Archimedes Foundation, DoRa scholarship EFS T6 – Development of international cooperation networks by supporting the mobility of Estonian doctoral students  
2009–2010 Skype and Estonian Information Technology Foundation, Skype foreign studies Master’s scholarship  
2008–2009 Archimedes Foundation, Kristjan Jaak scholarship for studying towards the Master’s degree in Engineering at the UNSW, Australia

**Supervised dissertations:**  
2015 Mirjam Põhjala, MSc, Supervisor MEng Aire Olesk, “Felling detection in Estonian forest using Sentinel-1A satellite images”

**Professional training:**

- 2014 MapInfo Training Course, Tartu, Estonia, 25 November 2014  
2013 2nd Advanced Course on Radar Polarimetry), ESA ESRIN, Italy, 21–25 January 2013  
2012 ESA Remote Sensing Course, participant and member of the organization committee, Tartu, Estonia, 16–20 April 2012

**Language skills:**

Estonian – native  
English – fluent  
Russian – basic  
German – basic  
Italian – basic

**Publications:**

- Olesk, A.**, Praks, J., Antropov, O., Arumäe, T., Zalite, K. and Voormansik, K., “Interferometric SAR Coherence Models for Characterization of Hemiboreal Forests using TanDEM-X Data,” *Remote Sensing*, vol. 8(9), pp. 700, 2016.
- Praks, J., **Olesk, A.**, Voormansik, K., Antropov, O., Zalite, K. and Noorma M., “Building blocks for semi-empirical models for forest parameter extraction from interferometric X-band SAR images,” In *Proceedings of the IEEE International Geoscience and Remote Sensing Symposium (IGARSS)*, pp. 736–739, 2016.
- Olesk, A.**, Voormansik, K., Põhjala, M. and Noorma, M., “Forest change detection from Sentinel-1 and ALOS-2 satellite images,” In *Proceedings of the IEEE 5th Asia-Pacific Conference on Synthetic Aperture Radar (APSAR)*, pp. 522–527, 2015.
- Olesk, A.**, Voormansik, K., Tamm, T., Noorma, M. and Praks, J., “Seasonal effects on the estimation of height of boreal and deciduous forests from interferometric TanDEM-X coherence data,” In *Proceedings of the SPIE Remote Sensing, International Society for Optics and Photonics*, pp. 964406–964406, 2015.
- Olesk, A.**, Voormansik, K., Vain, A., Noorma, M. and Praks, J., “Seasonal differences in forest height estimation from interferometric TanDEM-X coherence data,” *IEEE Journal of Selected Topics in Applied Earth Observations and Remote Sensing*, vol. 8, no. 12, pp. 5565–5572, 2015.
- Zalite, K., Voormansik, K., **Olesk, A.**, Noorma, M. and Reinart, A., “Effects of Inundated Vegetation on X-Band HH–VV Backscatter and Phase Difference,” *IEEE Journal of Selected Topics in Applied Earth Observations and Remote Sensing*, vol. 7, no. 4, pp. 1402–1406, 2014.
- Olesk, A.** and Voormansik, K., “Radarkaugseire rakendused metsanduses ning kasutusvõimalused metsa kõrguse kaardistamisel Eestis,” Aan, Anne; Narusk, Kirke (Eds.), *Kaugseire Eestis*, pp. 149–155, Estonian Environment Agency, 2014.

- Voormansik, K., Tamm, T., **Olesk, A.**, Zalite, K. and Praks, J. “Polarimeetrilise tehisava-radari kasutusvõimalustest Eesti keskkonnaseires RADARSAT-2 Rannu 2013. a andmestiku põhjal,” Aan, Anne; Narusk, Kirke (Eds.), *Kaugseire Eestis*, pp. 94–104, Estonian Environment Agency, 2014.
- Olesk, A.**, Voormansik, K., Luud, A., Rennel, M., Zalite, K., Noorma, M. and Reinart, A., “Countrywide Forest Biomass Estimates from PALSAR L-Band Backscatter To Improve Greenhouse Gas Inventory In Estonia,” In: L. Ouwehand, ESA Communications (Ed.). In *Proceedings of the ‘6th Int. Workshop on Science and Applications of SAR Polarimetry and Polarimetric Interferometry – PolInSAR* (ESA SP-713, August 2013) (128). ESA Publications Division, 2013.
- Voormansik, K., Jagdhuber, T., **Olesk, A.**, Hajnsek, I. and Papathanassiou K.P., “Towards a detection of grassland cutting practices with dual polarimetric TerraSAR-X data,” *International Journal of Remote Sensing*, vol. 34, no. 22, pp. 8081–8103, 2013.
- Nilson, T., Rennel, M., Luhamaa, A., Hordo, M., **Olesk, A.** and Lang, M., “MERIS GPP/NPP product for Estonia: I. Algorithm and preliminary results of simulation,” *Forestry Studies*, vol. 56, no. 1, pp. 56–78, 2012.

## CURRICULUM VITAE IN ESTONIAN

**Nimi:** Aire Olesk  
**Sünniaeg:** 16. detsember 1985, Jõgeva, Eesti  
**Kodakondsus:** Eesti  
**Aadress:** Tartu Observatoorium, 61602, Tõravere, Eesti  
**Telefon:** +372 5220939  
**E-mail:** aire@ut.ee

**Haridus:**  
2012–2016 Tartu Ülikool, doktorant  
2008–2011 New South Wales'i ülikool (Sydney, Austraalia), Geodeesia ja Ruumilised Infosüsteemid, MEng teadusmagister  
2005–2008 Tartu Ülikool, Geograafia, BSc

**Teenistuskäik:**  
2011–... Reach-U AS, projektijuht ja kaugseire spetsialist  
2013–... Tartu Observatoorium, Nooremteadur  
2012–2013 Euroopa Kosmoseagentuur (ESA-ESRIN), stažöör (National Trainee)  
2008–2011 Sensis (Sydney, Austraalia), geoinformaatik  
2006–2008 Regio AS, geoinformaatik ja välitöötaja

**Stipendiumid:**  
2015 SA Archimedes Kristjan Jaagu välissõidu stipendium  
2013 SA Archimedes Kristjan Jaagu välissõidu stipendium  
2012–2016 DoRa tegevus 3: doktoriõpe osaliselt väljaspool ülikooli (koostöös ettevõtetega)  
2012 DoRa tegevus 6: uurimistöö või õppekursuste läbimine välismaa ülikoolis/teadusasutuses  
2009–2010 Skype'i ja Eesti Infotehnoloogia Sihtasutuse magistristipendium õpinguteks New South Wales'i ülikoolis  
2008–2009 SA Archimedes Kristjan Jaagu stipendium, magistriõpinguteks New South Wales'i ülikoolis

**Juhendatud väitekirjad:**  
2015 Mirjam Põhjala, MSc, juhendaja MEng Aire Olesk, "Raiete tuvastamine Eesti metsades radarsatelliit Sentinel-1A abil"

**Täiendkoolitused:**  
2015 MapInfo kursus, Tartu, Eesti, 25. november, 2014  
2013 Radarpolarimeetria kursus (2nd Advanced Course on Radar Polarimetry), ESA ESRIN, Itaalia, 21.–25. jaanuar 2013  
2012 ESA Radarkaugseire kursus, osavõtja ja organiseerimiskomisjoni liige, Tartu, Eesti, 16.–20. aprill 2012

**Keeleoskus:**

eesti keel – emakeel  
inglise keel – väga hea  
vene keel – algtase  
saksa keel – algtase  
itaalia keel – algtase

**Publikatsioonid:**

- Olesk, A.**, Praks, J., Antropov, O., Arumäe, T., Zalite, K. and Voormansik, K., “Interferometric SAR Coherence Models for Characterization of Hemiboreal Forests using TanDEM-X Data,” *Remote Sensing*, vol. 8(9), pp. 700, 2016.
- Praks, J., **Olesk, A.**, Voormansik, K., Antropov, O., Zalite, K. and Noorma M., “Building blocks for semi-empirical models for forest parameter extraction from interferometric X-band SAR images,” In *Proceedings of the IEEE International Geoscience and Remote Sensing Symposium (IGARSS)*, pp. 736–739, 2016.
- Olesk, A.**, Voormansik, K., Põhjala, M. and Noorma, M., “Forest change detection from Sentinel-1 and ALOS-2 satellite images,” In *Proceedings of the IEEE 5th Asia-Pacific Conference on Synthetic Aperture Radar (APSAR)*, pp. 522–527, 2015.
- Olesk, A.**, Voormansik, K., Tamm, T., Noorma, M. and Praks, J., “Seasonal effects on the estimation of height of boreal and deciduous forests from interferometric TanDEM-X coherence data,” In *Proceedings of the SPIE Remote Sensing, International Society for Optics and Photonics*, pp. 964406–964406, 2015.
- Olesk, A.**, Voormansik, K., Vain, A., Noorma, M. and Praks, J., “Seasonal differences in forest height estimation from interferometric TanDEM-X coherence data,” *IEEE Journal of Selected Topics in Applied Earth Observations and Remote Sensing*, vol. 8, no. 12, pp. 5565–5572, 2015.
- Zalite, K., Voormansik, K., **Olesk, A.**, Noorma, M. and Reinart, A., “Effects of Inundated Vegetation on X-Band HH–VV Backscatter and Phase Difference,” *IEEE Journal of Selected Topics in Applied Earth Observations and Remote Sensing*, vol. 7, no. 4, pp. 1402–1406, 2014.
- Olesk, A.** and Voormansik, K., “Radarkaugseire rakendused metsanduses ning kasutusvõimalused metsa kõrguse kaardistamisel Eestis,” Aan, Anne; Narusk, Kirke (Toim.). *Kaugseire Eestis*, pp. 149–155, Keskkonnaagentuur, 2014.
- Voormansik, K., Tamm, T., **Olesk, A.**, Zalite, K. and Praks, J. “Polarimeetrilise tehisava-radari kasutusvõimalustest Eesti keskkonnaseires RADARSAT-2 Rannu 2013. a andmestiku põhjal” Aan, Anne; Narusk, Kirke (Toim.). *Kaugseire Eestis*, pp. 94–104, Keskkonnaagentuur, 2014.
- Olesk, A.**, Voormansik, K., Luud, A., Rennel, M., Zalite, K., Noorma, M. and Reinart, A., “Countrywide Forest Biomass Estimates From PALSAR L-Band Backscatter To Improve Greenhouse Gas Inventory In Estonia,” In: L. Ouwehand, ESA Communications (Ed.). In *Proceedings of the ‘6th Int. Workshop*

*on Science and Applications of SAR Polarimetry and Polarimetric Interferometry – PolInSAR* (ESA SP-713, August 2013) (128). ESA Publications Division, 2013.

Voormansik, K., Jagdhuber, T., **Olesk, A.**, Hajnsek, I. and Papathanassiou K. P., “Towards a detection of grassland cutting practices with dual polarimetric TerraSAR-X data,” *International Journal of Remote Sensing*, vol. 34, no. 22, pp. 8081–8103, 2013.

Nilson, T., Rennel, M., Luhamaa, A., Hordo, M., **Olesk, A.** and Lang, M., “MERIS’*e* GPP/NPP tulem Eesti jaoks: I. Algoritm ja mudelarvutuste esialgsed tulemused,” *Forestry Studies*, vol. 56, no. 1, pp. 56–78, 2012.

## DISSERTATIONES PHYSICAE UNIVERSITATIS TARTUENSIS

1. **Andrus Ausmees.** XUV-induced electron emission and electron-phonon interaction in alkali halides. Tartu, 1991.
2. **Heiki Sõnajalg.** Shaping and recalling of light pulses by optical elements based on spectral hole burning. Tartu, 1991.
3. **Sergei Savihhin.** Ultrafast dynamics of F-centers and bound excitons from picosecond spectroscopy data. Tartu, 1991.
4. **Ergo Nõmmiste.** Leelishalogeniidide röntgenelektronemissioon kiiritamisel footonitega energiaga 70–140 eV. Tartu, 1991.
5. **Margus Rätsep.** Spectral gratings and their relaxation in some low-temperature impurity-doped glasses and crystals. Tartu, 1991.
6. **Tõnu Pullerits.** Primary energy transfer in photosynthesis. Model calculations. Tartu, 1991.
7. **Olev Saks.** Attoampri diapsoonis voolude mõõtmise füüsikalised alused. Tartu, 1991.
8. **Andres Virro.** AlGaAsSb/GaSb heterostructure injection lasers. Tartu, 1991.
9. **Hans Korge.** Investigation of negative point discharge in pure nitrogen at atmospheric pressure. Tartu, 1992.
10. **Jüri Maksimov.** Nonlinear generation of laser VUV radiation for high-resolution spectroscopy. Tartu, 1992.
11. **Mark Aizengendler.** Photostimulated transformation of aggregate defects and spectral hole burning in a neutron-irradiated sapphire. Tartu, 1992.
12. **Hele Siimon.** Atomic layer molecular beam epitaxy of  $A^2B^6$  compounds described on the basis of kinetic equations model. Tartu, 1992.
13. **Tõnu Reinot.** The kinetics of polariton luminescence, energy transfer and relaxation in anthracene. Tartu, 1992.
14. **Toomas Rõõm.** Paramagnetic  $H^{2-}$  and  $F^+$  centers in CaO crystals: spectra, relaxation and recombination luminescence. Tallinn, 1993.
15. **Erko Jalviste.** Laser spectroscopy of some jet-cooled organic molecules. Tartu, 1993.
16. **Alvo Aabloo.** Studies of crystalline celluloses using potential energy calculations. Tartu, 1994.
17. **Peeter Paris.** Initiation of corona pulses. Tartu, 1994.
18. **Павел Рубин.** Локальные дефектные состояния в  $CuO_2$  плоскостях высокотемпературных сверхпроводников. Тарту, 1994.
19. **Olavi Ollikainen.** Applications of persistent spectral hole burning in ultrafast optical neural networks, time-resolved spectroscopy and holographic interferometry. Tartu, 1996.
20. **Ülo Mets.** Methodological aspects of fluorescence correlation spectroscopy. Tartu, 1996.
21. **Mikhail Danilkin.** Interaction of intrinsic and impurity defects in CaS:Eu luminophors. Tartu, 1997.

22. **Ирина Кудрявцева.** Создание и стабилизация дефектов в кристаллах KBr, KCl, RbCl при облучении ВУФ-радиацией. Тарту, 1997.
23. **Andres Osvet.** Photochromic properties of radiation-induced defects in diamond. Tartu, 1998.
24. **Jüri Örd.** Classical and quantum aspects of geodesic multiplication. Tartu, 1998.
25. **Priit Sarv.** High resolution solid-state NMR studies of zeolites. Tartu, 1998.
26. **Сергей Долгов.** Электронные возбуждения и дефектообразование в некоторых оксидах металлов. Тарту, 1998.
27. **Каupo Kukli.** Atomic layer deposition of artificially structured dielectric materials. Tartu, 1999.
28. **Ivo Heinmaa.** Nuclear resonance studies of local structure in  $\text{RBa}_2\text{Cu}_3\text{O}_{6+x}$  compounds. Tartu, 1999.
29. **Aleksander Shelkan.** Hole states in  $\text{CuO}_2$  planes of high temperature superconducting materials. Tartu, 1999.
30. **Dmitri Nevedrov.** Nonlinear effects in quantum lattices. Tartu, 1999.
31. **Rein Ruus.** Collapse of 3d (4f) orbitals in 2p (3d) excited configurations and its effect on the x-ray and electron spectra. Tartu, 1999.
32. **Valter Zazubovich.** Local relaxation in incommensurate and glassy solids studied by Spectral Hole Burning. Tartu, 1999.
33. **Indrek Reimand.** Picosecond dynamics of optical excitations in GaAs and other excitonic systems. Tartu, 2000.
34. **Vladimir Babin.** Spectroscopy of exciton states in some halide macro- and nanocrystals. Tartu, 2001.
35. **Toomas Plank.** Positive corona at combined DC and AC voltage. Tartu, 2001.
36. **Kristjan Leiger.** Pressure-induced effects in inhomogeneous spectra of doped solids. Tartu, 2002.
37. **Helle Kaasik.** Nonperturbative theory of multiphonon vibrational relaxation and nonradiative transitions. Tartu, 2002.
38. **Tõnu Laas.** Propagation of waves in curved spacetimes. Tartu, 2002.
39. **Rünno Lõhmus.** Application of novel hybrid methods in SPM studies of nanostructural materials. Tartu, 2002.
40. **Kaido Reivelt.** Optical implementation of propagation-invariant pulsed free-space wave fields. Tartu, 2003.
41. **Heiki Kasemägi.** The effect of nanoparticle additives on lithium-ion mobility in a polymer electrolyte. Tartu, 2003.
42. **Villu Repän.** Low current mode of negative corona. Tartu, 2004.
43. **Алексей Котлов.** Оксианионные диэлектрические кристаллы: зонная структура и электронные возбуждения. Tartu, 2004.
44. **Jaak Talts.** Continuous non-invasive blood pressure measurement: comparative and methodological studies of the differential servo-oscillometric method. Tartu, 2004.
45. **Margus Saal.** Studies of pre-big bang and braneworld cosmology. Tartu, 2004.

46. **Eduard Gerškevičš.** Dose to bone marrow and leukaemia risk in external beam radiotherapy of prostate cancer. Tartu, 2005.
47. **Sergey Shchemelyov.** Sum-frequency generation and multiphoton ionization in xenon under excitation by conical laser beams. Tartu, 2006.
48. **Valter Kiisk.** Optical investigation of metal-oxide thin films. Tartu, 2006.
49. **Jaan Aarik.** Atomic layer deposition of titanium, zirconium and hafnium dioxides: growth mechanisms and properties of thin films. Tartu, 2007.
50. **Astrid Rekker.** Colored-noise-controlled anomalous transport and phase transitions in complex systems. Tartu, 2007.
51. **Andres Punning.** Electromechanical characterization of ionic polymer-metal composite sensing actuators. Tartu, 2007.
52. **Indrek Jõgi.** Conduction mechanisms in thin atomic layer deposited films containing TiO<sub>2</sub>. Tartu, 2007.
53. **Aleksei Krasnikov.** Luminescence and defects creation processes in lead tungstate crystals. Tartu, 2007.
54. **Küllike Rägo.** Superconducting properties of MgB<sub>2</sub> in a scenario with intra- and interband pairing channels. Tartu, 2008.
55. **Els Heinsalu.** Normal and anomalously slow diffusion under external fields. Tartu, 2008.
56. **Kuno Kooser.** Soft x-ray induced radiative and nonradiative core-hole decay processes in thin films and solids. Tartu, 2008.
57. **Vadim Boltrushko.** Theory of vibronic transitions with strong nonlinear vibronic interaction in solids. Tartu, 2008.
58. **Andi Hektor.** Neutrino Physics beyond the Standard Model. Tartu, 2008.
59. **Raavo Josepson.** Photoinduced field-assisted electron emission into gases. Tartu, 2008.
60. **Martti Pärs.** Study of spontaneous and photoinduced processes in molecular solids using high-resolution optical spectroscopy. Tartu, 2008.
61. **Kristjan Kannike.** Implications of neutrino masses. Tartu, 2008.
62. **Vigen Issahhanjan.** Hole and interstitial centres in radiation-resistant MgO single crystals. Tartu, 2008.
63. **Veera Krasnenko.** Computational modeling of fluorescent proteins. Tartu, 2008.
64. **Mait Müntel.** Detection of doubly charged higgs boson in the CMS detector. Tartu, 2008.
65. **Kalle Kepler.** Optimisation of patient doses and image quality in diagnostic radiology. Tartu, 2009.
66. **Jüri Raud.** Study of negative glow and positive column regions of capillary HF discharge. Tartu, 2009.
67. **Sven Lange.** Spectroscopic and phase-stabilisation properties of pure and rare-earth ions activated ZrO<sub>2</sub> and HfO<sub>2</sub>. Tartu, 2010.
68. **Aarne Kasikov.** Optical characterization of inhomogeneous thin films. Tartu, 2010.
69. **Heli Valtna-Lukner.** Superluminally propagating localized optical pulses. Tartu, 2010.

70. **Artjom Vargunin.** Stochastic and deterministic features of ordering in the systems with a phase transition. Tartu, 2010.
71. **Hannes Liivat.** Probing new physics in  $e^+e^-$  annihilations into heavy particles via spin orientation effects. Tartu, 2010.
72. **Tanel Mullari.** On the second order relativistic deviation equation and its applications. Tartu, 2010.
73. **Aleksandr Lissovski.** Pulsed high-pressure discharge in argon: spectroscopic diagnostics, modeling and development. Tartu, 2010.
74. **Aile Tamm.** Atomic layer deposition of high-permittivity insulators from cyclopentadienyl-based precursors. Tartu, 2010.
75. **Janek Uin.** Electrical separation for generating standard aerosols in a wide particle size range. Tartu, 2011.
76. **Svetlana Ganina.** Hajusandmetega ülesanded kui üks võimalus füüsika-õppe efektiivsuse tõstmiseks. Tartu, 2011
77. **Joel Kuusk.** Measurement of top-of-canopy spectral reflectance of forests for developing vegetation radiative transfer models. Tartu, 2011.
78. **Raul Rammula.** Atomic layer deposition of  $\text{HfO}_2$  – nucleation, growth and structure development of thin films. Tartu, 2011.
79. **Сергей Наконечный.** Исследование электронно-дырочных и интерстициал-вакансионных процессов в монокристаллах  $\text{MgO}$  и  $\text{LiF}$  методами термоактивационной спектроскопии. Тарту, 2011.
80. **Niina Voropajeva.** Elementary excitations near the boundary of a strongly correlated crystal. Tartu, 2011.
81. **Martin Timusk.** Development and characterization of hybrid electro-optical materials. Tartu, 2012, 106 p.
82. **Merle Lust.** Assessment of dose components to Estonian population. Tartu, 2012, 84 p.
83. **Karl Kruusamäe.** Deformation-dependent electrode impedance of ionic electromechanically active polymers. Tartu, 2012, 128 p.
84. **Liis Rebane.** Measurement of the  $W \rightarrow \tau\nu$  cross section and a search for a doubly charged Higgs boson decaying to  $\tau$ -leptons with the CMS detector. Tartu, 2012, 156 p.
85. **Jevgeni Šablonin.** Processes of structural defect creation in pure and doped  $\text{MgO}$  and  $\text{NaCl}$  single crystals under condition of low or super high density of electronic excitations. Tartu, 2013, 145 p.
86. **Riho Vendt.** Combined method for establishment and dissemination of the international temperature scale. Tartu, 2013, 108 p.
87. **Peeter Piksarv.** Spatiotemporal characterization of diffractive and non-diffractive light pulses. Tartu, 2013, 156 p.
88. **Anna Šugai.** Creation of structural defects under superhigh-dense irradiation of wide-gap metal oxides. Tartu, 2013, 108 p.
89. **Ivar Kuusik.** Soft X-ray spectroscopy of insulators. Tartu, 2013, 113 p.
90. **Viktor Vabson.** Measurement uncertainty in Estonian Standard Laboratory for Mass. Tartu, 2013, 134 p.

91. **Kaupo Voormansik.** X-band synthetic aperture radar applications for environmental monitoring. Tartu, 2014, 117 p.
92. **Deivid Pugal.** hp-FEM model of IPMC deformation. Tartu, 2014, 143 p.
93. **Siim Pikker.** Modification in the emission and spectral shape of photo-stable fluorophores by nanometallic structures. Tartu, 2014, 98 p.
94. **Mihkel Pajusalu.** Localized Photosynthetic Excitons. Tartu, 2014, 183 p.
95. **Taavi Vaikjärv.** Consideration of non-adiabaticity of the Pseudo-Jahn-Teller effect: contribution of phonons. Tartu, 2014, 129 p.
96. **Martin Vilbaste.** Uncertainty sources and analysis methods in realizing SI units of air humidity in Estonia. Tartu, 2014, 111 p.
97. **Mihkel Rähn.** Experimental nanophotonics: single-photon sources- and nanofiber-related studies. Tartu, 2015, 107 p.
98. **Raul Laasner.** Excited state dynamics under high excitation densities in tungstates. Tartu, 2015, 125 p.
99. **Andris Slavinskis.** EST Cube-1 attitude determination. Tartu, 2015, 104 p.
100. **Karlis Zalite.** Radar Remote Sensing for Monitoring Forest Floods and Agricultural Grasslands. Tartu, 2016, 124 p.
101. **Kaarel Piip.** Development of LIBS for *in-situ* study of ITER relevant materials. Tartu, 2016, 93 p.
102. **Kadri Isakar.**  $^{210}\text{Pb}$  in Estonian air: long term study of activity concentrations and origin of radioactive lead. Tartu, 2016, 107 p.
103. **Artur Tamm.** High entropy alloys: study of structural properties and irradiation response. Tartu, 2016, 115 p.
104. **Rasmus Talviste.** Atmospheric-pressure He plasma jet: effect of dielectric tube diameter. Tartu, 2016, 107 p.
105. **Andres Tiko.** Measurement of single top quark properties with the CMS detector. Tartu, 2016, 161 p.